Synthesis, Reactivity, and Ring-Opening Polymerization (ROP) of Tin-Bridged [1]Ferrocenophanes

Frieder Jäkle, Ron Rulkens, Gernot Zech, Daniel A. Foucher, Alan J. Lough, and Ian Manners*

Abstract: The first examples of tin-bridged [1]ferrocenophanes, Fe(η-C_5H_4)$_2$-Sn*t*Bu$_2$ (**7a**) and Fe(η-C_5H_4)$_2$SnMes$_2$ (**7b**) have been synthesized by the low-temperature reaction of Fe(η-C_5H_4Li)$_2\cdot n$TMEDA (TMEDA = *N*,*N*,*N*′,*N*′-tetramethylethylenediamine) with *t*Bu$_2$SnCl$_2$ and Mes$_2$SnCl$_2$ (Mes = 2,4,6-trimethylphenyl), respectively. They were isolated in 65% (**7a**) and 85% (**7b**) yield as orange crystalline solids, which were characterized by multinuclear NMR and UV/Vis spectroscopy, mass spectrometry, elemental analysis, and single-crystal X-ray diffraction. The tilt angles between the planes of the cyclopentadienyl rings are 14.1(2)° for **7a** and 15.2(2)° (average) for the three independent molecules of **7b** in the unit cell. Although they have significantly smaller tilt angles than analogous [1]ferrocenophanes with the lighter Group 14 elements silicon or germanium in the bridge, **7a** and **7b** still readily undergo ring-opening polymerization (ROP) by thermal reaction in the solid state (**7a** at 150°C; **7b** at 180°C), to give high-molecular-weight poly(ferrocenylstannane)s [Fe(η-C_5H_4)$_2$Sn*t*Bu$_2$]$_n$ (**8a**) and [Fe(η-C_5H_4)$_2$SnMes$_2$]$_n$ (**8b**). Remarkably, **7a** and **7b** were also found to polymerize in solution at room temperature in the absence of externally added initiators. ROP is much more rapid for **7a** than for **7b** in solution. The cyclic dimers [Fe(η-C_5H_4)$_2$SnR$_2$]$_2$ (**3**; R = *t*Bu, Mes) were formed as by-products in amounts which depended on the solvent. Electrochemical studies of the cyclic dimers and polymers indicated the presence of significant Fe···Fe interactions that are mediated by the tin-atom spacer. When benzene solutions of **7a** and **7b** were treated with small amounts of Karstedt's catalyst, *slower* polymerization was observed. Stoichiometric reaction of Pt(1,5-cod)$_2$ (cod = cyclooctadiene) with **7a** yielded the novel trimetallic 1-stanna-2-platina[2]ferrocenophane Fe(η-C_5H_4)$_2$Pt(1,5-cod)Sn*t*Bu$_2$ (**9**), which functioned as a sluggish catalyst for the ROP of **7a** and **7b**.

Keywords: [1]ferrocenophanes · metallocenes · poly(ferrocene) · ring-opening polymerization · tin

Introduction

Transition-metal-based polymers are attracting attention as processable materials with interesting properties and potential applications.[1, 2] Thermal, anionic, cationic, and transition-metal-catalyzed ring-opening polymerization (ROP) of strained, ring-tilted [1]ferrocenophanes **1** and their analogues (for example, [2]ferrocenophanes) is a versatile route to a variety of high-molecular-weight ($M_n > 10^5$) poly(metallocene)s **2** and related materials.[3] The resulting polymers have generated interest as precursors to magnetic materials (including nanostructures), which are obtained from them by pyrolysis or oxidation; their electrochromic, conformational, and morphological characteristics (including liquid crystallinity), and their interesting charge-transport properties (which are a result of metal–metal interactions) have all been subjects of recent research.[4, 5]

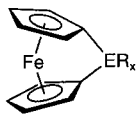

1

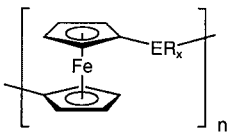

2

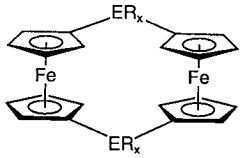

3

It is remarkable that, even as recently as 1970, [1]ferrocenophanes such as **1** (ER$_x$ = SiR$_2$) were considered too strained to exist.[6] The first [1]ferrocenophane, the silicon-bridged species **1** (ER$_x$ = SiPh$_2$), was synthesized successfully and

[*] Prof. I. Manners, Dr. F. Jäkle, Dr. R. Rulkens, G. Zech, Dr. A. J. Lough
Department of Chemistry, University of Toronto
80 St. George Street, Toronto, Ontario, M5S 3H6 (Canada)
Fax: (+1) 416 978-6157
E-mail: imanners@alchemy.chem.utoronto.ca
Dr. D. A. Foucher
Xerox Research Centre of Canada
2660 Speakman Drive, Mississauga, Ontario, L5K 2L1 (Canada)

  0947-6539/98/0411-2117 $ 17.50+.25/0

characterized in 1975 by Osborne and co-workers. The synthetic procedure involved a low-temperature reaction of dilithioferrocene·*n*TMEDA with Ph_2SiCl_2.[7] In the subsequent 20 years a range of analogous species with Group 14 (Si, Ge)[8], Group 15 (P, As)[8–10], and Group 4 (Ti, Zr, Hf)[11, 12] bridging elements were isolated. These molecules all possess strained structures with ring tilts between the planes of the cyclopentadienyl ligands (α) of 6–27° and angles between the *ipso*-C–E bonds and the planes of cyclopentadienyl ligands (β) of 28.8–40.1°, and have attracted attention because of their interesting reactivity and their ability to function as surface-derivatization reagents (for example, for silica) as well as their use as ROP monomers.[3a, 4a, 4f] As the properties of the ring-opened organometallic materials **2** are modified significantly by the nature of the spacer ER_x, the extension of the range of [1]ferrocenophanes by incorporation of other bridging elements is of considerable interest.[13–15] The first [1]ferrocenophanes containing Group 16 (S, Se)[16] or Group 13 (B)[17] elements in the bridge were reported very recently. These novel, highly strained species (ring tilts 26–32°) also undergo ROP. The metal–metal interactions in the case of poly(metallocene)s **2** ($ER_x = S$) with a single sulfur spacer appear to be the strongest detected so far on the basis of redox coupling measured by cyclic voltammetry.[16]

Although they have large covalent radii, which would be expected to lead to less intrinsic ring strain, the introduction of elements below the fourth period as bridging atoms for [1]ferrocenophanes is synthetically challenging because of the weakness of the bonds between *ipso*-carbon and the bridging element. Thus, although [1]ferrocenophanes containing Group 14 elements Si and Ge in the bridge are well known,[8] previous attempts to synthesize stanna[1]ferrocenophanes by the reaction of dilithioferrocene·*n*TMEDA with diorganodichlorostannanes R_2SnCl_2 (R = Me, Et, *n*Bu, Ph) were unsuccessful and resulted only in the isolation of oligomers **2** ($ER_x = SnR_2$; R = Me, Et, *n*Bu, Ph; $M_n < 4600$) and cyclic dimers **3** ($ER_x = SnR_2$; R = Et, Bu).[8–9, 18] The absence of a stanna[1]ferrocenophane in the product mixture was attributed to the high reactivity of the Sn–Cl bonds, which might favor *inter*molecular condensation reactions over *intra*molecular cyclizations.[18] In contrast, the synthesis of essentially unstrained metallocenophanes containing 2–3 and 1 tin atom(s) in the *ansa*-bridge has been described for ferrocene- and zirconocene-based systems, respectively. Thus, Herberhold et al. recently synthesized the first distanna[2]ferrocenophane (**4**) and tristanna[3]ferrocenophane (**5**).[19] The structure of **4** was determined; its tilt angle was found to be 0.7°. Furthermore Herrmann et al. found the *ansa*-tin-bridged zirconocene **6** to be a good catalyst for ethylene polymerization.[20]

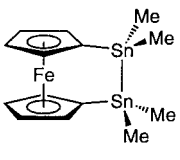

4

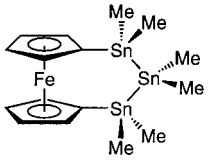

5

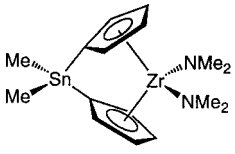

6

In a recent communication we reported the first successful synthesis and characterization of a tin-bridged [1]ferrocenophane (**7a**; Scheme 1) by using sterically demanding *tert*-butyl

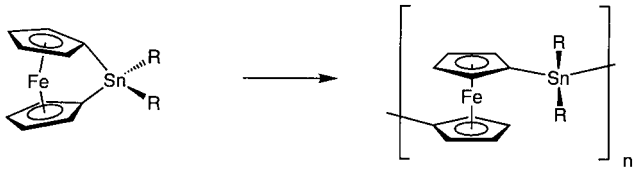

7 **8**

Scheme 1. Stanna[1]ferrocenophanes and their ROP.

substituents at tin.[21] In this paper we give full details of the synthesis and structural characterization of this species and an analogue (**7b**) and describe the polymerization behavior and properties of the resulting ring-opened poly(ferrocenylstannane) materials (**8a**, **8b**).[22, 23]

Results and Discussion

Synthesis and characterization of the tin-bridged [1]ferrocenophanes 7a and 7b

*Synthesis of **7a** and **7b***: Initially we attempted to isolate a tin-bridged [1]ferrocenophane from the low-temperature reaction of dilithioferrocene·*n*TMEDA with nBu_2SnCl_2 in Et_2O.[24] Although a color change from amber to orange was detected below −40 °C, warming the reaction mixture led to amber oligomeric products similar to those previously reported.[18] In particular, the known cyclic dimer $[Fe(\eta\text{-}C_5H_4)_2SnnBu_2]_2$ and low-molecular-weight polymer $[Fe(\eta\text{-}C_5H_4)_2SnnBu_2]_n$ ($M_n = 6100$, PDI = 2.3) were identified by ^1H, ^{13}C, and ^{119}Sn NMR, and the latter also by gel permeation chromatography (GPC). We expected the presence of bulkier substituents to stabilize a stanna[1]ferrocenophane, so we studied the reaction of dilithioferrocene·*n*TMEDA with tBu_2SnCl_2 in diethyl ether. At −35 °C the reaction mixture showed a subtle color change from amber to orange. When it had reached −30 °C it was warmed rapidly to 20 °C and filtered to remove LiCl. The filtrate was collected at −78 °C to avoid spontaneous polymerization of the product; at this temperature orange needles of the first stanna[1]ferrocenophane (**7a**) were formed, which were isolated in 65% yield. We explored the analogous reaction between dilithioferrocene·*n*TMEDA and Mes_2SnCl_2 (Mes = 2,4,6-trimethylphenyl). The change to mesityl substituents on tin made it possible to work up the reaction mixture at ambient temperature. After removal of the solvent a solid orange residue was obtained, which was dried in vacuo (10^{-3} mm Hg) for 12 h to ensure that no traces of TMEDA were left in the crude product. Recrystallization from Et_2O/hexanes (1:3) gave orange-red crystals of **7b** in 85% yield. Further efforts to prepare isolable stanna[1]ferrocenophanes by reaction of dilithioferrocene·*n*TMEDA with $nBuMesSnCl_2$, PhMes-

0947-6539/98/0411-2118 $ 17.50+.50/0 *Chem. Eur. J.* **1998**, *4*, No. 11

$SnCl_2$, or $MesSnCl_3$ were unsuccessful. Although there was NMR spectroscopic evidence for monomer formation, attempts to purify the crude product always led to oligomeric material. It therefore appears that the presence of *two* sterically demanding substituents on tin is important to avoid ring-opening reactions during the product work-up.

Characterization of ***7a*** *and* ***7b***: ^{1}H, ^{13}C, ^{119}Sn NMR, UV/Vis spectroscopy, and mass spectrometry confirmed the assigned structures of **7a** and **7b**. NMR and UV/Vis spectroscopy indicated a less strained structure for **7a** and **7b** compared with the Si and Ge analogues **1** ($ER_2 = SiMe_2$ and $GeMe_2$; see Table 1).[25] For example, the ^{1}H NMR spectrum (in $CDCl_3$) of **7b** shows a pair of far less widely separated pseudotriplets ($\delta = 4.23$ and 4.36) assigned to the α and β Cp protons. Thus the splitting between the pseudotriplets, $\Delta\delta$, is 0.13, 0.22, 0.26, and 0.40 for **7b**, **7a**, **1** ($ER_2 = GeMe_2$), and **1** ($ER_2 = SiMe_2$), respectively. In the ^{13}C NMR spectrum the *ipso*-Cp resonances of **7a** and **7b** at $\delta = 34.9$ and 38.2 appear at slightly lower fields than those of **1** (E = Si, Ge), but are still extremely shielded compared with those of unstrained ferrocene derivatives.

Crystals of tin-bridged [1]ferrocenophane **7a** that were suitable for an X-ray diffraction study were obtained by low-temperature (below $-20\,^\circ$C) recrystallization from Et_2O/THF (10:1), whereas single crystals of **7b** were grown from Et_2O/hexanes (1:3) at $-55\,^\circ$C. Crystals of **7b** contain three different molecules in the unit cell (designated **7b^{I}**, **7b^{II}**, **7b^{III}**). The three independent molecules of **7b** differ mainly in the position of their mesityl rings relative to the ferrocene core: by rotation of the mesityl substituents around the Sn–C(Mes) bond, different conformers are obtained. The molecular structures of **7a** and **7b^{I}** are shown in Figures 1 and 2 and selected bond lengths and angles are listed in Tables 2 and 3. The most important structural features indicating ring strain are the tilt angle α (**7a**: 14.1(2)°; **7b^{I}**: 15.3(2); **7b^{II}**: 14.5(2); **7b^{III}**: 15.7(3)°) and the angle β (**7a**: 36.2(2), 36.1(2)°; **7b^{I}**: 35.2(2), 35.3(2); **7b^{II}**: 36.2(2), 35.4(2); **7b^{III}**: 35.7(2), 35.1(2)°). The tilt angles α for **7a** and **7b** are the smallest yet reported for a [1]ferrocenophane with a main-group element in the

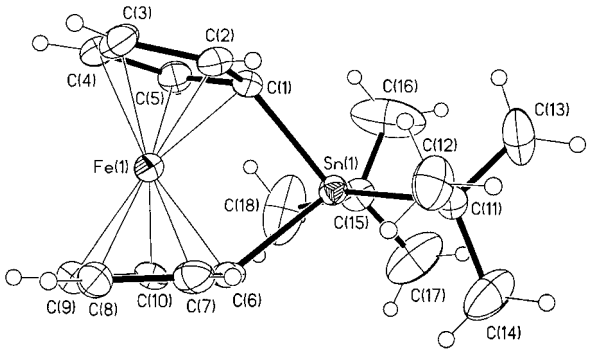

Figure 1. Molecular structure of **7a** with thermal ellipsoids at the 30% probability level.

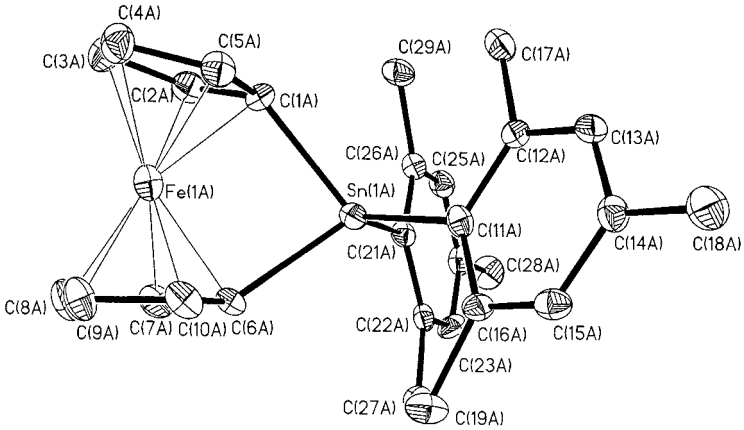

Figure 2. Molecular structure of **7b^{I}** with thermal ellipsoids at the 30% probability level.

Table 2. Selected bond lengths [Å] and angles [°] for **7a**.

Sn(1)–C(6)	2.171(5)	Fe(1)–C(3)	2.059(5)	C(7)–C(8)	1.414(9)
Sn(1)–C(1)	2.174(4)	Fe(1)–C(4)	2.062(5)	C(8)–C(9)	1.401(11)
Sn(1)–C(11)	2.180(5)	Fe(1)–C(9)	2.063(6)	C(9)–C(10)	1.414(8)
Sn(1)–C(15)	2.190(6)	Fe(1)–C(8)	2.068(5)		
Sn(1)–Fe(1)	2.9761(8)	C(1)–C(5)	1.423(7)	C(6)-Sn(1)-C(1)	86.5(2)
Fe(1)–C(2)	2.026(5)	C(1)–C(2)	1.427(7)	C(6)-Sn(1)-C(11)	111.9(2)
Fe(1)–C(5)	2.027(5)	C(2)–C(3)	1.416(8)	C(1)-Sn(1)-C(11)	114.9(2)
Fe(1)–C(7)	2.027(5)	C(3)–C(4)	1.400(8)	C(6)-Sn(1)-C(15)	114.6(2)
Fe(1)–C(1)	2.036(5)	C(4)–C(5)	1.437(7)	C(1)-Sn(1)-C(15)	110.6(2)
Fe(1)–C(10)	2.036(6)	C(6)–C(7)	1.432(7)	C(11)-Sn(1)-C(15)	115.1(2)
Fe(1)–C(6)	2.041(5)	C(6)–C(10)	1.446(8)		

Table 3. Selected bond lengths [Å] and angles [°] for **7b^{I}**.

Sn(1)–C(6)	2.159(4)	Fe(1)–C(3)	2.060(4)	C(7)–C(8)	1.415(5)
Sn(1)–C(1)	2.162(4)	Fe(1)–C(4)	2.048(4)	C(8)–C(9)	1.418(6)
Sn(1)–C(11)	2.168(4)	Fe(1)–C(9)	2.064(4)	C(9)–C(10)	1.409(6)
Sn(1)–C(21)	2.167(4)	Fe(1)–C(8)	2.068(5)		
Sn(1)–Fe(1)	2.9859(7)	C(1)–C(5)	1.416(5)	C(6)-Sn(1)-C(1)	85.7(2)
Fe(1)–C(2)	2.020(4)	C(1)–C(2)	1.428(6)	C(6)-Sn(1)-C(11)	111.3(2)
Fe(1)–C(5)	2.022(4)	C(2)–C(3)	1.431(5)	C(1)-Sn(1)-C(11)	110.9(2)
Fe(1)–C(7)	2.029(4)	C(3)–C(4)	1.403(6)	C(6)-Sn(1)-C(21)	114.1(2)
Fe(1)–C(1)	2.027(4)	C(4)–C(5)	1.418(6)	C(1)-Sn(1)-C(21)	114.4(2)
Fe(1)–C(10)	2.027(4)	C(6)–C(7)	1.434(6)	C(11)-Sn(1)-C(21)	116.5(1)
Fe(1)–C(6)	2.034(4)	C(6)–C(10)	1.444(5)		

Table 1. Comparison of data indicating ring strain in group 14 bridged [1]ferrocenophanes.

	α [°]	β[a] [°]	$\lambda_{max.}$[b] [nm]	ε [$M^{-1}cm^{-1}$]	δ(*ipso*-C)[c] [ppm]	$\Delta\delta$ H(Cp)[d] [ppm]
1 ($ER_2 = SiMe_2$)	20.8(5)	37.0(6)	481	341	33.1	0.40
1 ($ER_2 = GeMe_2$)	19.0(9)	36.8(5)	420/486	75/283	30.0	0.26
7a	14.1(2)	36.2(2)	418/485	75/158	34.9	0.22
7b	15.2(2)[a]	35.3(2)	420/481	90/176	38.2	0.13
Fe(η-$C_5H_4SiMe_3$)$_2$	0	0	448	130	72.0	0.22

[a] Average values; [b] 1.1×10^{-3} M in THF; [c] ^{13}C NMR spectra in $CDCl_3$; [d] ^{1}H NMR spectra in $CDCl_3$.

bridge and are significantly less than for silicon- and germanium-bridged analogues (Table 1). Cp ring tilting is accompanied by an RC(1)-Fe-RC(2) (RC = ring centroid) angle of 168.6(2)° for **7a** and 167.5(2), 168.0(2), 167.3(2)° for the three conformers of **7b**, compared with 180° in ferrocene. In addition, a significant displacement of the iron atom from the line joining the two ring centroids is apparent (**7a**: 0.164(6) Å; **7b**: 0.179(4), 0.172(4), 0.182(4) Å). The tilted Cp rings maintain an eclipsed conformation. The angle between the Cp *ipso*-C–Sn bonds (C1-Sn-C6), θ, is 86.5(2)° for **7a** and 85.7(2)°, 85.9(1)°, 85.9(1)° for the conformers of **7b**; this is significantly smaller than the analogous angles for **1** ($ER_2 = SiMe_2$) and **1** ($ER_2 = GeMe_2$) where θ = 95.7(4)° and 91.7(3)°, respectively. The average Sn–C bond lengths (**7a**: Sn–C_{Cp} = 2.173(4); **7b**: Sn–C_{Cp} = 2.166(4); Sn–C_{tBu} = 2.185(5); Sn–C_{Mes} = 2.163(4) Å) are typical for Sn–C single bonds. The Sn–Fe distances of **7a** (2.9761(8) Å) and **7b** (average value: 2.9900(7) Å) are only 14–18% longer than iron–tin bond lengths found in the species $CpL_2Fe–SnR_3$ (2.537–2.605 Å).[26] This suggests the possible occurrence of significant overlap of the iron and tin orbitals to give a weak bond.[27]

In THF there are two absorptions for **7a** in the visible region at 418 nm ($\varepsilon_{max} = 75\,M^{-1}cm^{-1}$) and at 485 nm ($\varepsilon_{max} = 158\,M^{-1}cm^{-1}$) (Figure 3); for **7b** very

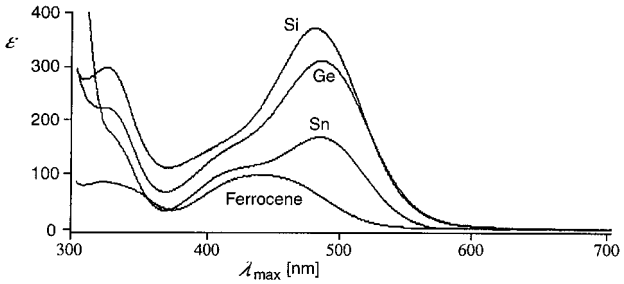

Figure 3. UV/Vis spectra (in THF) of ferrocene and Group 14-bridged [1]ferrocenophanes. From top to bottom: **1** ($ER_x = SiMe_2$), **1** ($ER_x = GeMe_2$), **7a**, and ferrocene.

similar absorptions are observed [$\lambda_{max} = 420$ ($\varepsilon_{max} = 90\,M^{-1}cm^{-1}$) and 481 nm ($\varepsilon_{max} = 176\,M^{-1}cm^{-1}$)]. For comparison, two overlapping bands, which can be resolved at low temperatures, are present in the visible spectrum of ferrocene at 417 nm ($\varepsilon_{max} = 72\,M^{-1}cm^{-1}$) and at 459 nm ($\varepsilon_{max} = 36\,M^{-1}cm^{-1}$) which are assigned to the electronic transitions $^1A_{1g} \rightarrow {}^1E_{1g}$ and $^1A_{1g} \rightarrow {}^1E_{2g}$, respectively.[28] The red-shift of the longer-wavelength band of **7a** and **7b** relative to that of ferrocene is typical for strained Group 14 [1]ferrocenophanes (Table 1). The extent of the bathochromic shift does not seem to depend on the ring tilt α alone since the λ_{max} values are all relatively close to one another. However, the absorption coefficient of the $^1A_{1g} \rightarrow {}^1E_{2g}$ transition increases with ring tilt α and varies from $36\,M^{-1}cm^{-1}$ for ferrocene to 158/176, 283, and $341\,M^{-1}cm^{-1}$ for the tin-, germanium-, and silicon-bridged [1]ferrocenophane, respectively (Table 1).[29] That the ε_{max} values of the $^1A_{1g} \rightarrow {}^1E_{2g}$ electronic transitions are higher than that of ferrocene indicates a distortion of the inversion symmetry of the ferrocene unit, which makes the g–g electronic transition allowed.[29]

ROP of stanna[1]ferrocenophanes 7a and 7b

*Synthesis and characterization of the poly(ferrocenylstannane)s **8a** and **8b***: In order to investigate whether **7a** and **7b** undergo a thermally induced ROP similarly to other [1]ferrocenophanes **1** (E = Si, Ge, P, S, B), we studied the thermal behavior of these compounds by differential scanning calorimetry (DSC) (see Figure 4). When heated above 150 °C,

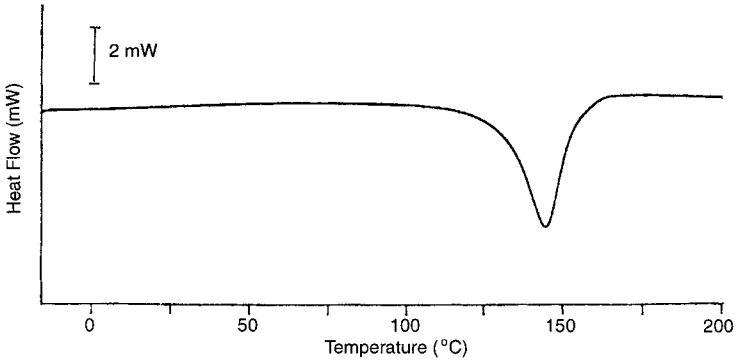

Figure 4. DSC of the polymerization of **7a** (5.8 mg; heating rate 10 °C min^{-1}).

the samples did not show any endotherm corresponding to a melt, but instead a single exotherm which indicated an ROP reaction in the solid state.[30] By integration of the ROP exotherm we found that **7a** has an approximate strain energy of 36 ± 9 kJ mol^{-1}, which is slightly higher than that of **7b** (18 ± 10 kJ mol^{-1}). These enthalpies of polymerization found by DSC analysis are significantly smaller than those obtained for the ROP of silicon-bridged [1]ferrocenophanes (70–80 kJ mol^{-1}) and Group 16 element-bridged [1]ferrocenophanes (110–130 kJ mol^{-1}), which is consistent with their less strained structures.[3a, 16, 31]

Surprisingly, **7a** and **7b** are stable to air for several days in the solid state. After prolonged storage (approximately four weeks) of **7a** in air at room temperature a poly(ferrocenylstannane) with a broad, bimodal molecular weight distribution had formed (high-molecular-weight fraction: M_w = 231 000, M_n = 130 000, PDI = 1.8; low-molecular-weight fraction: M_w = 15 000, M_n = 5000, PDI = 3.0). Compound **7a** was therefore stored at −40 °C under N_2. When **7a** was heated in the solid state at 150 °C for 30 min, the amber poly(ferrocenylstannane) **8a** was formed.[30] This material was soluble in fairly polar and aromatic organic solvents (for example, THF, CH_2Cl_2, or toluene) and was characterized by ^1H, ^{13}C, and ^{119}Sn NMR spectroscopy and elemental analysis. In addition, analysis of the molecular weight distribution by GPC in THF against polystyrene standards showed that the material was of high molecular weight (M_w = 133 000, M_n = 83 000, PDI = 1.6). Remarkably, when **7a** was dissolved in toluene, quantitative ROP occurred at room temperature over 6 h to form high-molecular-weight **8a** (M_w = 900 000, M_n = 560 000, PDI = 1.6).

Even at low conversion (approximately 20%, after 1 h) high-molecular-weight polymer (M_w = 630 000, M_n = 480 000,

0947-6539/98/0411-2120 $ 17.50+.50/0 *Chem. Eur. J.* **1998**, *4*, No. 11

PDI = 1.3) was formed, indicating that the ROP is a chain-growth process. However, when **7a** was dissolved in $CHCl_3$ a much lower-molecular-weight polymer **8a** ($M_w = 10000$, $M_n = 4700$, PDI = 2.2) and the cyclic dimer **3** ($ER_x = SntBu_2$) (see below) were formed over a similar 6 h period.

In contrast to **7a**, the dimesityl-substituted species **7b** did not show any tendency to polymerize at ambient temperature in air in the solid state. To obtain complete transformation to polymeric material, **7b** had to be heated for more than 6 h at 180 °C. A similar trend was observed for the polymerization in solution of **7b** compared with **7a**. Thus, in contrast to **7a**, after 6 h the conversion of **7b** to cyclic oligomer **3** ($ER_x = SnMes_2$) and polymeric material **8b** in solution (C_6D_6 or $CDCl_3$) was less than 3% as detected by ^1H NMR spectroscopy. Even after 30 days at 25 °C a substantial amount (more than 30%) of monomer was still left. As observed with **7a**, the highest molecular weights were obtained from the polymerization of **7b** in benzene ($M_w = 1350000$, $M_n = 1050000$, PDI = 1.3 after 15 days and 50% conversion), whereas thermal polymerization in the solid state gave lower-molecular-weight polymer ($M_w = 155000$, $M_n = 82000$, PDI = 1.9) and in $CDCl_3$ solution at 25 °C cyclic dimer **3** was the main product. In the latter case GPC ($M_n < 1000$ after 15 days and 50% conversion) and ^1H NMR data (broad singlet at $\delta = 4.10$, indicative of an unsubstituted Cp ring) suggest the formation of very low-molecular-weight material as a by-product, which is probably owing to decomposition pathways involving reaction with $CDCl_3$.

It is noteworthy that the exact molecular weights as well as the polydispersities of polymers **8a** and **8b** vary from sample to sample and from experiment to experiment, for both thermal polymerization in the solid state and polymerization in solution at 25 °C. The polymerization of **7b** in benzene, for example, gave materials with M_w from 800000 to 1500000 and with a PDI of 1.3–1.6. Furthermore, prolonged storage in solution in the presence of light and air can lead to partial precipitation and to different molecular weights as determined by GPC analysis.

In order to investigate the morphology of polymers **8a** and **8b**, wide-angle X-ray scattering (WAXS) was performed on thermally polymerized single crystals of **7a** and on a purified sample of **8b**, which was precipitated twice from toluene solution into hexanes. Whereas the diffractogram of **8a** showed several sharp peaks, indicating that the material is semi-crystalline, that of **8b** displayed only an amorphous halo.

Characterization of the cyclic dimers ***3*** *($ER_x = SntBu_2$) and* ***3*** *($ER_x = SnMes_2$)*: As mentioned above, during the solution polymerization of **7a** and **7b** the cyclic dimers **3** ($ER_x = SntBu_2$) and **3** ($ER_x = SnMes_2$), respectively, were formed as side products. The maximum amount of **3** ($ER_x = SntBu_2$) was found to be formed in CH_2Cl_2 (25 °C; yield approximately 50% by ^1H NMR spectroscopy), whereas refluxing in $CHCl_3$ was required to obtain a substantial amount of **3** ($ER_x = SnMes_2$) within a reasonable reaction time (yield approximately 30% after 1 day according to ^1H NMR spectroscopy and GPC analysis). The orange crystalline cyclic dimers **3** were isolated in approximately 20–30% yield (based on **7**) by flash chromatography and recrystallization from toluene. In the mixture of products in $CDCl_3$ the cyclic dimers **3** were easily distinguished from the stanna[1]ferrocenophanes **7** and poly(ferrocenylstannane)s **8** by NMR spectroscopy. Thus, the *t*Bu groups in the ^1H NMR spectrum of **3** ($ER_x = SntBu_2$) are slightly more shielded than those of **7a** and **8a** ($\delta = 1.18$, compared with $\delta = 1.48$ and 1.34 respectively). Similarly, in the ^1H NMR spectrum of **3** ($ER_x = SnMes_2$) the methyl groups in the *ortho* position of the mesityl substituents appear at higher field than those of **7b**, but at lower field than in **8b** ($\delta = 2.25$, compared with $\delta = 2.71$ and 2.10 respectively). The steric requirements of the mesityl groups in **3** ($ER_x = SnMes_2$) lead to a broadening of the Cp-H(2,5) ^1H NMR signal, which is most probably due to rotational hindrance. In the ^{13}C NMR spectra, the splitting between the Cp (CH) resonances for **3** ($ER_x = SntBu_2$) and **3** ($ER_x = SnMes_2$) is larger than those for **7a,b** and **8a,b** ($\Delta\delta = 5.0$ and 5.7 compared with $\Delta\delta = 2.2$ and 1.3 for **7a,b** and $\Delta\delta = 3.4$ and 2.8 for **8a,b**). The chemical shift of the ^{119}Sn NMR resonance of **3** ($ER_x = SntBu_2$) lies between those of **7a** and **8a** ($\delta = -33.3$ compared with $\delta = -23.7$ and -45.2, respectively). In contrast, a significant high-field shift is observed for the ^{119}Sn NMR signal of **3** ($ER_x = SnMes_2$) compared with both monomeric **7b** and polymeric **8b** ($\delta = -111.5$ compared with $\delta = -128.3$ and -127.0, respectively).

Crystals of the cyclic dimers **3** ($ER_x = SntBu_2$ and $SnMes_2$) that were suitable for a single-crystal X-ray diffraction study were obtained by slow evaporation of toluene solvent from a solution and by recrystallization from hot toluene (100 °C), respectively. The molecular structures of **3** are shown in Figures 5 and 6 and selected bond lengths and angles are given

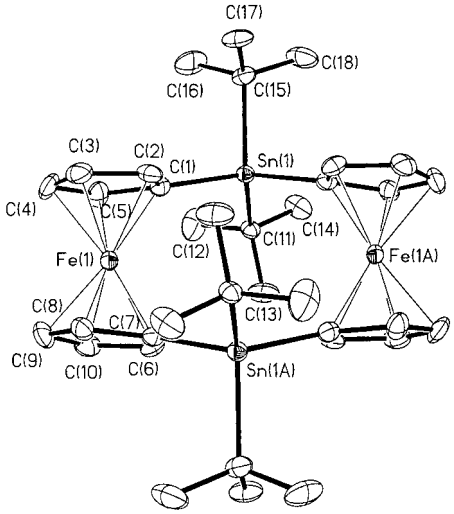

Figure 5. Molecular structure of **3** ($ER_x = SntBu_2$) with thermal ellipsoids at the 30% probability level.

in Tables 4 and 5. The tin-bridged [1,1]ferrocenophanes **3** ($ER_x = SntBu_2$ and $SnMes_2$) exhibit a chair-like *anti* conformation similar to the silicon-bridged [1,1]ferrocenophane **3** ($ER_x = SiMe_2$).[32, 33] Remarkably, the tilt angles α and β, although small, are opposite in direction to those in [1]ferrocenophanes. Thus for **3** ($ER_x = SntBu_2$ and $SnMes_2$) ring tilts α of $-5.0(2)^\circ$ and $-3.3(2)^\circ$ are observed and the β angles are $-11.2(2)^\circ$, $-9.6(2)^\circ$, and $-8.0(2)^\circ$, $-7.9(2)^\circ$, respectively. For

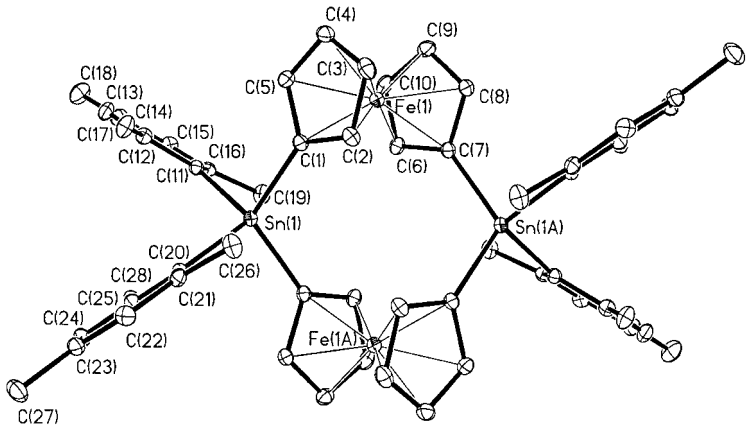

Figure 6. Molecular structure of **3** ($ER_x = SnMes_2$) with thermal ellipsoids at the 30% probability level.

Table 4. Selected bond lengths, interatomic distances [Å] and angles [°] for **3** ($ER_x = SntBu_2$).[a]

Sn(1)−C(7)#1	2.135(3)	Fe(1)−C(5)	2.056(4)	C(8)−C(9)	1.433(5)
Sn(1)−C(1)	2.148(3)	Fe(1)−C(7)	2.076(3)	C(9)−C(10)	1.406(6)
Sn(1)−C(11)	2.196(3)	Fe(1)−C(1)	2.077(3)	Fe(1)···Sn(1)	3.947(1)
Sn(1)−C(15)	2.202(4)	C(1)−C(2)	1.428(5)	Fe(1)···Fe(1)#1	5.474(1)
Fe(1)−C(9)	2.038(4)	C(1)−C(5)	1.442(5)		
Fe(1)−C(8)	2.038(3)	C(2)−C(3)	1.426(5)	C(7)#1-Sn(1)-C(1)	110.91(13)
Fe(1)−C(4)	2.042(4)	C(3)−C(4)	1.421(6)	C(7)#1-Sn(1)-C(11)	113.36(13)
Fe(1)−C(3)	2.043(4)	C(4)−C(5)	1.428(6)	C(1)-Sn(1)-C(11)	113.10(13)
Fe(1)−C(10)	2.049(4)	C(6)−C(7)	1.432(5)	C(7)#1-Sn(1)-C(15)	102.03(13)
Fe(1)−C(2)	2.050(3)	C(6)−C(10)	1.435(5)	C(1)-Sn(1)-C(15)	102.51(13)
Fe(1)−C(6)	2.052(4)	C(7)−C(8)	1.439(5)	C(11)-Sn(1)-C(15)	113.91(13)

[a] Symmetry transformations used to generate equivalent atoms: #1 $-x+1, -y+1, -z+1$.

Table 5. Selected bond lengths, interatomic distances [Å] and angles [°] for **3** ($ER_x = SnMes_2$).[a]

Sn(1)−C(7)#1	2.149(2)	Fe(1)−C(5)	2.039(2)	C(8)−C(9)	1.419(3)
Sn(1)−C(1)	2.143(2)	Fe(1)−C(7)	2.075(2)	C(9)−C(10)	1.412(3)
Sn(1)−C(11)	2.178(2)	Fe(1)−C(1)	2.066(2)	Fe(1)···Sn(1)	3.750(1)
Sn(1)−C(20)	2.178(2)	C(1)−C(2)	1.439(3)	Fe(1)···Fe(1)#1	5.248(1)
Fe(1)−C(9)	2.045(2)	C(1)−C(5)	1.439(3)		
Fe(1)−C(8)	2.045(2)	C(2)−C(3)	1.419(3)	C(7)#1-Sn(1)-C(1)	117.55(8)
Fe(1)−C(4)	2.051(2)	C(3)−C(4)	1.416(3)	C(7)#1-Sn(1)-C(11)	118.66(7)
Fe(1)−C(3)	2.066(2)	C(4)−C(5)	1.421(3)	C(1)-Sn(1)-C(11)	100.32(7)
Fe(1)−C(10)	2.043(2)	C(6)−C(7)	1.436(3)	C(7)#1-Sn(1)-C(20)	98.78(7)
Fe(1)−C(2)	2.044(2)	C(6)−C(10)	1.430(3)	C(1)-Sn(1)-C(20)	117.48(8)
Fe(1)−C(6)	2.047(2)	C(7)−C(8)	1.433(3)	C(11)-Sn(1)-C(20)	104.22(7)

[a] Symmetry transformations used to generate equivalent atoms: #1 $-x+1, -y+1, -z+1$.

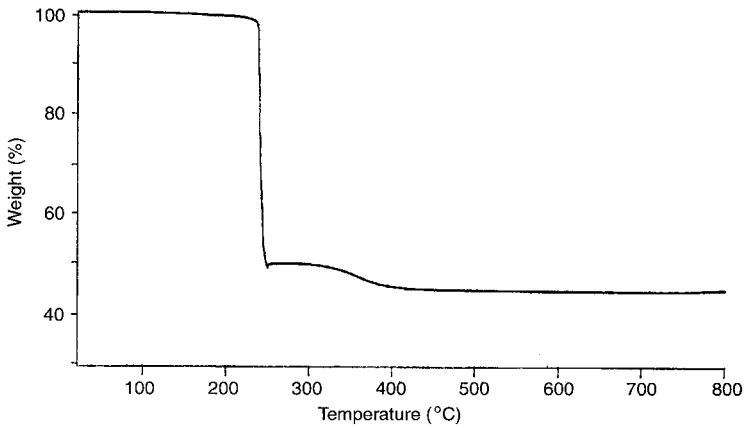

Figure 7. TGA of **8a** (4.2 mg; heating rate: 10 °C min^{-1}).

comparison, for **3** ($ER_x = SiMe_2$) $\alpha = 4.9(3)°$ and the β angles are $-7.8(8)°$ and $-7.4(8)°$.[33] The cyclopentadienyl ligands of the ferrocene units are staggered by 6.9(5)° and 6.4(5)°, as defined by the torsion angle C(1)-RC1-Fe-RC2-C(10) (RC = ring centroid) and the SnR_2 bridges are staggered by very similar angles of 65.0(5)° and 65.8(5)°. The Fe···Fe distance for **3** ($ER_x = SntBu_2$; 5.474(1) Å) is similar to that in **3** ($ER_x = SnnBu_2$; 5.50 Å), but longer than for the mesityl derivative **3** ($ER_x = SnMes_2$; 5.248(1) Å), in which the Fe···Fe distance is almost as short as in the related silicon-bridged species **3** ($ER_x = SiMe_2$; 5.171(9) Å), but longer than for **3** ($ER_x = CH_2$; d(Fe···Fe) = 4.816(2) Å).

*Thermal analysis of poly(ferrocenylstannane)s **8a** and **8b***: A polymer sample **8a**, formed by thermal ROP, was studied by DSC: its T_g was 124 °C. No melt transition was found for poly(ferrocenylstannane) **8a**, but above 210 °C an onset corresponding to exothermic decomposition of **8a** was observed. TGA under N_2 confirmed that **8a** decomposed above 210 °C: a sharp 50% weight loss at 235 °C and a further 5% weight loss between 300 and 400 °C resulted in the formation of a red-gold ceramic in a yield of 44% by weight at 900 °C (Figure 7). Poly(ferrocenylstannane) **8a** is therefore less thermally stable than poly(ferrocenylsilane)s, which do not undergo weight loss under nitrogen until approximately 350 °C.[34] These results are in sharp contrast with the thermal properties of polymer **8b**. As expected from the more rigid and bulky substituents on tin, the DSC trace of **8b** displays a much higher T_g of 208 °C (Figure 8). According to the TGA data, decomposition of **8b** resulting in significant weight loss takes place only above 320 °C. Between this temperature and 400 °C a 61% weight loss is observed; a golden ceramic is formed that does not undergo any further weight loss up to 900 °C.

^{57}Fe Mössbauer spectroscopic studies and electrochemical characterization of 3, 7a, 7b, 8a, and 8b

*^{57}Fe Mössbauer spectroscopic studies of **7a**, **3** ($R = SntBu_2$), and **8a***: It has been proposed that the reduced quadrupole splitting (Q.S.) of [1]ferrocenophanes bridged by Group 14 elements, compared with that of ferrocene, results from a dative bond between the iron and the bridging atom.[27a] The Q.S. for **7a** is larger than that of **1** ($ER_x = GeMe_2$), which is itself larger than that of **1** ($ER_x = SiMe_2$) (Table 6), possibly suggesting a decreasing tendency of iron to form a bond with the heavier Group 14 bridging atoms. The observed order might be explained by the fact that the tilt angle α is much bigger for the Ge- and Si-bridged [1]ferrocenophanes than for **7** according to their X-ray analyses (see Table 1), bringing the bridging unit closer to the central iron

  0947-6539/98/0411-2122 $ 17.50+.50/0 *Chem. Eur. J.* **1998**, *4*, No. 11

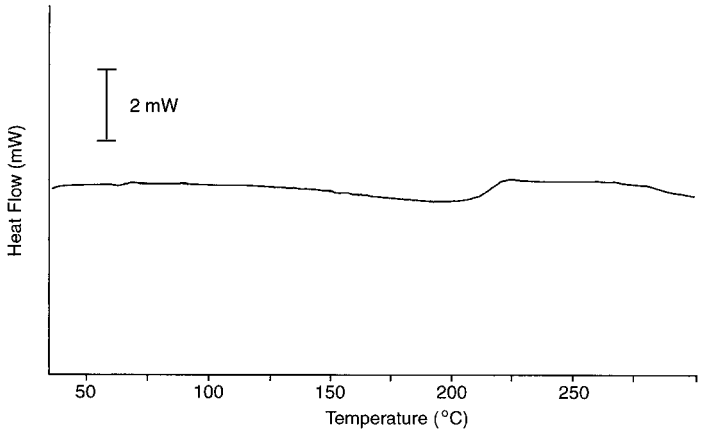

Figure 8. DSC of **8b** (14.3 mg; heating rate: 20 °C min^{-1}).

Table 6. Mössbauer data of selected group 14 bridged [1]ferrocenophanes, [1,1]ferrocenophanes and of polymers **2** ($ER_x = SiMe_2$) and **8a** recorded at room temperature.

	δ[mm s^{-1}][a]	Q.S. [mm s^{-1}]	reference
1 ($ER_x = SiMe_2$)	0.51	1.92	[35]
1 ($ER_x = GeMe_2$)	0.33	2.10	[27b]
7a	0.46	2.14	This work
3 ($ER_x = SiMe_2$)	0.44	2.32	[33]
3 ($ER_x = SntBu_2$)	0.50	2.32	This work
8a	0.49	2.33	This work
2 ($ER_x = SiMe_2$)	0.41	2.35	[36]
Ferrocene	0.51	2.37	[8b]

[a] δ = isomer shift.

atom. Accordingly, the Q.S. increases from the monomer **7a** to the dimeric species **3** ($ER_x = SntBu_2$), to the polymer **8a** and to the silicon-based polymer **2** ($ER_x = SiMe_2$); the value for **2** approaches that for ferrocene (2.37 mm s^{-1}). On the basis of the interpretation by Silver,[27a] this would indicate a small and decreasing interaction between the iron and the bridging atom.

*Electrochemical studies of **3** ($ER_x = SntBu_2$ and $SnMes_2$), **7a**, **7b**, **8a**, and **8b***: The ferrocenophanes **3** ($ER_x = SntBu_2$ and $SnMes_2$), **7a** and **7b**, and the poly(ferrocenylstannane)s **8a** and **8b** were studied by cyclic voltammetry, which was performed on samples containing 1.0 mg mL^{-1} of the ferrocenophane in 0.1 M solution of $[Bu_4N][PF_6]$ in CH_2Cl_2 at 20 °C, unless otherwise stated. The stanna[1]ferrocenophanes **7a** and **7b** undergo reversible one-electron oxidation ($E_{1/2} = -0.01$ V for both compounds versus ferrocene/ferrocenium), as found previously for silicon-bridged [1]ferrocenophanes.[35] Analysis of **8a** and **8b** by cyclic voltammetry showed the presence of two reversible oxidation waves (**8a**: $E_{1/2}$ = of 0.00 and 0.24 V versus the ferrocene/ferrocenium ion couple, redox coupling $\Delta E_{1/2} = 0.24$ V; **8b** (in THF): $E_{1/2} = -0.07$ and 0.14 V, $\Delta E_{1/2} = 0.21$ V) consistent with the presence of significant bridge-mediated interactions between the iron atoms.[2g, 3a, 4a, 15, 36–38] For tin-bridged [1,1]ferrocenophane **3** ($ER_x = SntBu_2$) two reversible waves at -0.06 and 0.21 V versus ferrocene/ferrocenium were found. In comparison, **3** ($ER_x = SnMes_2$) is reversibly oxidized at slightly higher potentials (0.01 and 0.29 V). The redox coupling for **3** ($ER_x = SntBu_2$: $\Delta E_{1/2} = 0.27$ V; $ER_x = SnMes_2$: $\Delta E_{1/2} = 0.28$ V) is thereby more pronounced than that found by Dong et al. for **3** ($ER_x = SnnBu_2$).[13] $\Delta E_{1/2}$ values for **3** ($ER_x = CH_2$, $SiMe_2$, $SntBu_2$, and $PbPh_2$) are 0.20, 0.25, 0.27, and 0.28 V, respectively. Significantly, although the Fe···Fe distance increases from E = Si to E = Pb for these [1,1]ferrocenophanes, the electrochemical interaction between the iron atoms still increases (Table 7). This indicates that a bridge-mediated interaction predominates over a direct coulombic through-space interaction.

Table 7. Redox-splitting ($\Delta E_{1/2}$) and intramolecular Fe–Fe distances for some [1.1]ferrocenophanes.

Compound **3** ER_x =	$\Delta E_{1/2}$[a] [V]	d (Fe···Fe) [Å]	reference
CH_2	0.20	4.816(2)	[39]
$SiMe_2$	0.25	5.171(9)	[33]
$SnnBu_2$	0.20	5.50	[13]
$SntBu_2$	0.27	5.474(1)	this work
$SnMes_2$	0.28	5.248(1)	this work
$PbPh_2$	0.28	–	[40]

[a] All values reported were obtained by analysis of CH_2Cl_2 solutions of analyte.

Attempted transition-metal-catalyzed ROP of 7a and 7b and synthesis and characterization of 9

*Attempted Pt^0-catalyzed ROP of **7a** and **7b***: To investigate whether **7a** would undergo transition-metal-catalyzed ROP in a similar manner to that established for **1** ($ER_x = SiMe_2$ and $GeMe_2$), the reaction of tin-bridged [1]ferrocenophane **7a** was attempted with two Pt^0 reagents that are known to catalyze the ROP of **1** ($ER_x = SiMe_2$) effectively.[41] Karstedt's catalyst, $Pt_2(\eta\text{-}CH_2CHSiMe_2OSiMe_2\eta\text{-}CHCH_2)_3$, appeared to *inhibit* the ROP polymerization of **7a** and **7b**. When **7a** was treated with a stoichiometric amount of $Pt(1,5\text{-cod})_2$ (cod = cyclooctadiene), which has recently been found to insert in the Si–*ipso*-C bond of **1** (E = $SiMe_2$) to form a 1-sila-2-platina[2]-ferrocenophane,[42] slow conversion (over 2 h) led to the formation of the platinum–tin-bridged [2]ferrocenophane **9** (Scheme 2).[43] The insertion product **9** was characterized by

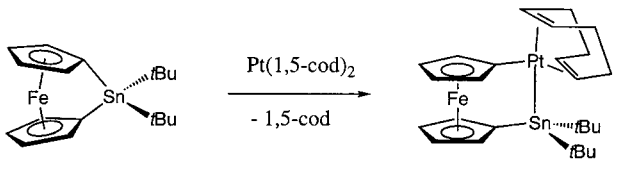

7a **9**

Scheme 2. Synthesis of **9**.

^{1}H, ^{13}C, ^{119}Sn, and ^{195}Pt NMR spectroscopy, mass spectrometry, elemental analysis, and X-ray crystallography. Significant NMR spectral features of **9** are the large ^{195}Pt–^{119}Sn coupling found in both the ^{195}Pt and ^{119}Sn NMR spectra (14640 Hz) and the 1055 Hz ^{195}Pt–^{13}C coupling between the *ipso*-C atom of the cyclopentadienyl ligand and platinum. When a small amount of 1-stanna-2-platina[2]ferrocenophane **9** reacted with **7a**, slow ROP (over 5 days) was observed.

X-ray structure of 1-stanna-2-platina[2]ferrocenophane ***9***: Crystals of tin–platinum-bridged [2]ferrocenophane **9** that were suitable for an X-ray diffraction study were obtained by recrystallization from toluene/hexanes (1:4). The molecular structure of **9** is shown in Figure 9 and selected bond lengths

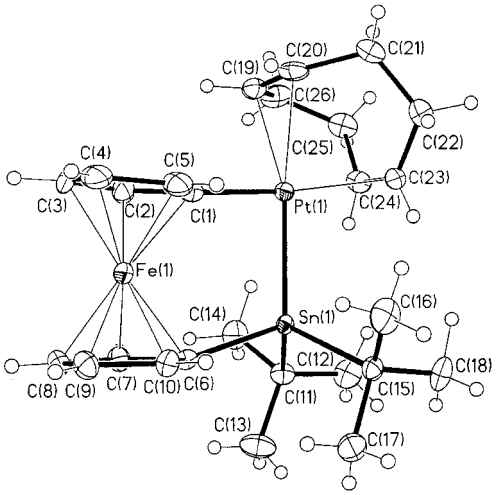

Figure 9. Molecular structure of **9** with thermal ellipsoids at the 30% probability level.

and angles are given in Table 8. The tilt angle α is 5.7(3)°, which is considerably less than that for **7a** and **7b**. Remarkably, the β angle on Pt is $-6.6(2)°$, whereas the β angle on Sn is 15.8(2)°. Thus the platinum is bent away from the iron atom, whereas the tin atom seems to be pulled towards it. A possible but speculative explanation involves the formation of a weak Fe–Sn bond by a dative interaction from the iron atom to the Lewis-acidic tin atom.[27b] The Sn···Fe distance of **9** is 3.461(1) Å, which is 0.485(1) Å longer than that in the stanna-[1]ferrocenophane **7a**, but 0.486(1) Å shorter than that in **3** ($ER_x = SntBu_2$). Analogous interactions have been proposed to account for the stability of ferrocene-substituted carbocations (bending of the carbenium moiety out of the Cp plane towards the central iron atom which was also found for the isoelectronic boryl-substituted ferrocenes).[44] The RC1-Fe-RC2 (RC = ring centroid) angle is 174.7(4)° and the displacement of the iron atom from the line joining the two ring centroids is 0.075(4) Å. The staggering angle between the Cp rings is 2.6(3)°, so there is only slight distortion from an eclipsed conformation. The Sn–C bond lengths are 2.163(3) Å for $Sn-C_{Cp}$ and 2.217(4) and 2.211(4) Å for $Sn-C_{tBu}$ and are very close to those found for **7a**. The Sn–Pt distance in **9** is 2.6065(4) Å, which is in the expected range for Pt–Sn bonds.[45]

Table 8. Selected bond lengths, interatomic distances [Å] and angles [°] for **9**.

Pt(1)–C(1)	2.034(4)	Fe(1)–C(5)	2.042(4)	C(1)-Pt(1)-C(23)	159.4(2)
Pt(1)–C(23)	2.229(4)	Fe(1)–C(9)	2.054(4)	C(1)-Pt(1)-C(24)	162.8(2)
Pt(1)–C(24)	2.264(4)	Fe(1)–C(8)	2.057(4)	C(1)-Pt(1)-C(19)	88.71(14)
Pt(1)–C(19)	2.320(4)	Fe(1)–C(1)	2.066(3)	C(1)-Pt(1)-C(20)	91.48(14)
Pt(1)–C(20)	2.339(4)	C(19)–C(20)	1.363(6)	C(1)-Pt(1)-Sn(1)	85.82(9)
Pt(1)–Sn(1)	2.6065(4)	C(19)–C(26)	1.506(6)	C(23)-Pt(1)-Sn(1)	97.97(10)
Sn(1)–C(6)	2.163(3)	C(20)–C(21)	1.524(6)	C(24)-Pt(1)-Sn(1)	101.06(10)
Sn(1)–C(11)	2.211(4)	C(21)–C(22)	1.541(6)	C(19)-Pt(1)-Sn(1)	159.11(10)
Sn(1)–C(15)	2.217(4)	C(22)–C(23)	1.512(6)	C(20)-Pt(1)-Sn(1)	166.04(11)
Fe(1)–C(10)	2.031(4)	C(23)–C(24)	1.385(6)	C(6)-Sn(1)-C(11)	103.42(14)
Fe(1)–C(7)	2.032(4)	C(24)–C(25)	1.506(6)	C(6)-Sn(1)-C(15)	104.79(13)
Fe(1)–C(2)	2.036(4)	C(25)–C(26)	1.533(7)	C(11)-Sn(1)-C(15)	112.10(14)
Fe(1)–C(4)	2.037(4)	Fe(1)···Sn(1)	3.461(1)	C(6)-Sn(1)-Pt(1)	108.74(9)
Fe(1)–C(3)	2.037(4)	Fe(1)···Pt(1)	3.770(1)	C(11)-Sn(1)-Pt(1)	112.99(10)
Fe(1)–C(6)	2.041(3)			C(15)-Sn(1)-Pt(1)	113.86(9)

Conclusion

The first examples of stanna[1]ferrocenophanes, **7a** and **7b**, have been synthesized by the reaction of tBu_2SnCl_2 and Mes_2SnCl_2 with dilithioferrocene·*n*TMEDA. These species possess ring tilts of 14–15° and represent the least ring-tilted [*n*]metallocenophanes that have so far been shown to undergo ROP. The alkyl-substituted ferrocenophane **7a** polymerizes thermally in the solid state, and even in solution at room temperature without the addition of initiator, to form high-molecular-weight poly(ferrocenylstannane)s **8a** in toluene. In chlorinated solvents such as $CHCl_3$ or CH_2Cl_2 the cyclic dimer **3** ($ER_x = SntBu_2$) and low-molecular-weight polymer **8a** form. In contrast to **7a**, the mesityl-substituted ferrocenophane **7b** polymerizes at 25 °C only very slowly in solution and is stable in the solid state, not forming any **8b** over a period of more than a month. The solution conversion of stanna[1]ferrocenophanes **7a** and **7b** to polymeric **8a** and **8b** is inhibited by Pt^0 species that function as catalysts for the ROP of analogous silicon-bridged species. However, with stoichiometric amounts of $Pt(1,5\text{-cod})_2$ the novel trimetallic 1-stanna-2-platina[2]ferrocenophane **9** was formed. Electrochemical studies on the dimeric species **3** indicate a dominant bridge-mediated interaction rather than a direct coulombic through-space interaction between the two different iron centers.

The observed ambient-temperature ROP of tin-bridged [1]ferrocenophanes and apparent inhibition by Pt^0 species is particularly intriguing. Detailed mechanistic studies of these ROP reactions are in progress and our results will be reported in the near future.

Experimental Section

Materials and methods: The compounds tBu_2SnCl_2, nBu_2SnCl_2, $nBuSnCl_3$, $PhSnCl_3$, and TMEDA were purchased from Aldrich. tBu_2SnCl_2, nBu_2SnCl_2, $nBuSnCl_3$, and $PhSnCl_3$ were used without further purification. TMEDA was distilled from Na before use. Dilithioferrocene·*n*TMEDA was synthesized according to a literature procedure.[46–48] The selective synthesis of Mes_2SnCl_2,[49, 50] $MesSnCl_3$,[49, 51] $nBuMesSnCl_2$, and $PhMesSnCl_2$ will be described elsewhere.[52] All reactions and manipulations were carried out under an atmosphere of prepurified nitrogen with use of either Schlenk techniques or an inert-atmosphere glove box (Vacuum Atmospheres) except for the purification of the polymers, which was carried out in air. Solvents were dried by standard methods and distilled before use. ^1H NMR spectra at 200, 300, or 400 MHz and ^{13}C NMR spectra at 50.3, 75.5, or 100.5 MHz were recorded either on a Varian XL200, Varian XL300, or Unity 400 spectrometer, respectively. The 111.8 MHz ^{119}Sn and 64.2 MHz ^{195}Pt NMR spectra were recorded on a Varian XL300 spectrometer. All solution ^1H and ^{13}C NMR spectra were referenced externally to TMS. ^{119}Sn spectra were referenced externally to $SnMe_4$ and ^{195}Pt NMR spectra were referenced to $\Theta =$ 21.4 MHz with $K_2Pt(CN)_6$ as external standard. Mass spectra were obtained

0947-6539/98/0411-2124 $ 17.50+.50/0 *Chem. Eur. J.* **1998**, *4*, No. 11

with a VG 70-250S mass spectrometer operating in electron impact (EI) mode for **3**, **7a, 7b**, **8a**, and **8b** and in fast atom bombardment (FAB) mode for **9**. The molecular weight of the polymers was estimated by GPC with a Waters Associates liquid chromatograph equipped with a 510 HPLC pump, U6K injector, ultrastyragel columns with a pore size between 10^3 and 10^5 Å, and a Waters 410 differential refractometer. The flow rate was 1.0 mL min^{-1}, and the sample was dissolved in a solution of [nBu$_4$N]Br (0.1 %) in THF. Polystyrene standards were used for calibration purposes. Elemental analyses were performed by Quantitative Technologies, Whitehouse (NJ). Wide-angle X-ray scattering data were obtained with a Siemens D 5000 diffractometer employing Ni-filtered Cu$_{K\alpha}$ ($\lambda = 1.54178$ Å) radiation. The samples were scanned at step widths of 0.02° for 1.2 s per step in the range $5° > 2\theta > 90°$. Samples for the X-ray studies were prepared by spreading the finely ground polymer on grooved polyethylene slides. Cyclic voltammetry was carried out with a Model 273 potentiostat/galvanostat (EG&G Princeton Applied Research) on solutions containing the sample (1.0 mg mL^{-1}) in a 0.10 M solution of [NBu$_4$][PF$_6$] in CH_2Cl_2. The sample cell had Pt working and counter electrodes and a silver reference electrode. Decamethylferrocene was added as an internal standard at the end of each experiment. In this paper, however, potentials are referred to the ferrocene/ferrocenium couple, which is 550 mV anodic relative to decamethylferrocene. UV/Vis spectra, DSC, and TGA data were obtained as previously described.[16b]

Reaction of dilithioferrocene · 2/3 TMEDA with nBu$_2$SnCl$_2$: A solution of nBu$_2$SnCl$_2$ (2.90 g, 9.54 mmol) in diethyl ether (50 mL) was added dropwise to a suspension of dilithioferrocene · 2/3 TMEDA (2.62 g, 9.54 mmol) in diethyl ether (100 mL) that was cooled to −78 °C. The reaction mixture was warmed slowly to 20 °C and vacuum-filtered through a fritted glass disk. From the filtrate the amber crystalline cyclic dimer **3** (R = nBu)[18] (1.2 g, 30 %) was isolated, and precipitation into hexanes afforded the amber, gummy low-molecular-weight polymer [FcSnnBu$_2$]$_n$ (**8c**) (1.6 g, 40 %). For **8c**: ^{1}H NMR (300 MHz, C_6D_6, 20 °C): $\delta = 4.35$ (br, 4H; Cp), 4.20 (br, 4H; Cp), 1.64–1.53 (m, 8H; $CH_2CH_2CH_2CH_3$), 1.13 (m, 4H; $CH_2CH_2CH_2CH_3$), 1.05 (m, 6H; $CH_2CH_2CH_2CH_3$); ^{13}C NMR (75.5 MHz, C_6D_6, 20 °C): $\delta =$ 74.8 ($J(^{117/119}\mathrm{Sn},\ ^{13}\mathrm{C}) = 23$ Hz; Cp), 71.4 ($J(^{117/119}\mathrm{Sn},^{13}\mathrm{C}) = 19$ Hz; Cp), 69.2 ($J(^{119}\mathrm{Sn},^{13}\mathrm{C}) = 233$ Hz, $J(^{117}\mathrm{Sn},^{13}\mathrm{C}) = 223$ Hz; *ipso*-Cp), 29.7 ($J(^{117/119}\mathrm{Sn},\ ^{13}\mathrm{C}) = 10$ Hz; $CH_2CH_2CH_2CH_3$), 27.9 ($J(^{117/119}\mathrm{Sn},^{13}\mathrm{C}) = 30$ Hz; $CH_2CH_2CH_2CH_3$), 14.3 ($CH_2CH_2CH_2CH_3$), 12.0 ($J(^{119}\mathrm{Sn},^{13}\mathrm{C}) = 193$ Hz, $J(^{117}\mathrm{Sn},\ ^{13}\mathrm{C}) = 184$ Hz; $CH_2CH_2CH_2CH_3$); ^{119}Sn NMR (111.8 MHz, C_6D_6, 20 °C): $\delta = -25.9$; GPC (THF, versus polystyrene): $M_n = 6100$ (PDI = 2.3).

Synthesis of stanna[1]ferrocenophane 7a: A solution of tBu$_2$SnCl$_2$ (2.32 g, 7.64 mmol) in diethyl ether (20 mL) was added dropwise to a suspension of dilithioferrocene · 2/3 TMEDA (2.00 g, 7.27 mmol) in diethyl ether (100 mL) that was cooled to −78 °C. The reaction mixture was warmed slowly to −30 °C, then rapidly to 20 °C, and vacuum-filtered through a fritted glass disk. Collection of the orange filtrate at −78 °C resulted in precipitation of the orange product. The mixture was cooled for 30 min at −78 °C, then the solvent was decanted off and the product was dried under vacuum. Analytically pure orange crystalline needles of stanna[1]ferrocenophane **7a** (1.98 g, 65 %) were isolated. ^{1}H NMR (300 MHz, $CDCl_3$, −20 °C): $\delta = 4.44$ (pst, J(H,H) = 2 Hz, 4H; Cp), 4.22 (pst, J(H,H) = 2 Hz, 4H; Cp), 1.48 (s/d, $J(^{117/119}\mathrm{Sn},\mathrm{H}) = 75$ Hz, 18H; tBu); ^{13}C NMR (75.5 MHz, $CDCl_3$, −20 °): $\delta = 77.9$ ($J(^{117/119}\mathrm{Sn},^{13}\mathrm{C}) = 28$ Hz; Cp), 75.7 ($J(^{117/119}\mathrm{Sn},^{13}\mathrm{C}) =$ 26 Hz; Cp), 34.9 (*ipso*-Cp), 32.8 (*ipso*-tBu), 31.8 (tBu); ^{119}Sn NMR (111.8 MHz, $CDCl_3$, −20 °C): $\delta = -23.7$; UV/Vis (THF): λ_{max} (ε) = 340 (sh), 418 (75), 485 (158); MS (70 eV, EI): *m/z* (%): 418 (62) [M^+], 361 (28) [$M^+ - t$Bu], 304 (100) [$M^+ - 2t$Bu], 248 (46) [$M^+ - 2t$BuFe], 186 (54) [Fe($\eta - C_5H_5)_2^+$]; $C_{18}H_{26}$FeSn (416.9): calcd C 51.85, H 6.29; found C 51.51, H 6.29; DSC: polymerization exotherm 145 °C (peak), 130 °C (onset), $\Delta H = -36(9)$ kJ mol^{-1}.

ROP of 7a and synthesis of 8a: The poly(ferrocenylstannane) **8a** was obtained from **7a** in two ways.

Thermal ROP: Solid-state polymerization was carried out by heating crystalline **7a** (typically 2.0 g) in a sealed, evacuated Pyrex tube at 150 °C for 30 min. Monomodal high-molecular-weight poly(ferrocenylstannane) **8a** was formed in a quantitative yield.

ROP in solution: When **7a** (50 mg, 0.12 mmol) was dissolved in $CDCl_3$ (0.5 mL) at 20 °C, it underwent complete conversion over 3 h to the cyclic dimer **3** (30 %) and to polymeric material **8a** (70 %), which was isolated by precipitation into hexanes and was shown to have a low molecular weight. In toluene, high-molecular-weight polymer **8a** and only a small amount (<5 %) of dimer **3** were formed. For **8a**: ^{1}H NMR (300 MHz, $CDCl_3$, 20 °C): $\delta = 4.24$ (pst, J(H,H) = 2 Hz, 4H; Cp), 3.97 (pst, J(H,H) = 2 Hz, 4H; Cp), 1.34 (s/d, $J(^{117/119}\mathrm{Sn},\mathrm{H}) = 65$ Hz, 18H; tBu); ^{13}C NMR (75.5 MHz, $CDCl_3$, 20 °C): $\delta = 74.5$ ($J(^{117/119}\mathrm{Sn},^{13}\mathrm{C}) = 24$ Hz; Cp), 71.1 ($J(^{117/119}\mathrm{Sn},^{13}\mathrm{C}) =$ 32 Hz; Cp), 70.6 (*ipso*-Cp), 31.8 (tBu), 29.0 (*ipso*-tBu); ^{119}Sn NMR (111.8 MHz, $CDCl_3$, 20 °C): $\delta = -45.2$; pyrolysis MS (70 eV, EI, 250 °C): *m/z* (%): 242 (12) [Fe(η-C_5H_5)(η-C_5H_4tBu)$^+$], 186 (100) [Fe(η-$C_5H_5)_2^+$]; pyrolysis MS (70 eV, EI, 375 °C): *m/z* (%): 660 (8) [(η-C_5H_5)Fe(η-C_5H_4SntBu$_2\eta$-C_5H_4)Fe(η-C_5H_4tBu)$^+$] [M^+], 604 (12) [MH$^+ - t$Bu], 546 (17) [$M^+ - 2t$Bu], 490 (10) [$M^+ - 3t$Bu], 426 (15) [$M^+ - 3t$Bu − Cp], 298 (57) [Fe(η-C_5H_4tBu)$_2^+$], 242 (71) [Fe(η-C_5H_5)(η-C_5H_4tBu)$^+$], 186 (100) [Fe(η-$C_5H_5)_2^+$]; UV/Vis (THF): λ_{max} (ε) = 340 (sh), 452 (152); [$C_{18}H_{26}$FeSn]$_n$ ([416.9]$_n$): calcd C 51.85, H 6.29; found C 51.86, H 6.37; DSC: $T_g = 124$ °C ($\Delta C_p = 28(5)$ J mol^{-1}), $T_{dec} = 210$ °C; GPC (THF, versus polystyrene): thermal polymerization $M_n = 83000$ (PDI = 1.6); polymerization in solution (20 °C): $CHCl_3$, $M_n = 4700$ (PDI = 2.2); toluene, $M_n = 560000$ (PDI = 1.6). The WAXS pattern of **8a** (from single crystals of **7a** polymerized at 150 °C) displayed sharp peaks at d spacings of 17.68, 13.99, 11.82, 8.568, 7.403, 7.060, 6.915, 5.865, 4.838, 3.859, 3.391, and 3.092 Å.

Synthesis of 7b: A suspension of Mes$_2$SnCl$_2$ (1.33 g, 3.11 mmol) in diethyl ether (40 mL) was added dropwise to a suspension of dilithioferrocene · 2/3 TMEDA (0.85 g, 3.09 mmol) in diethyl ether (100 mL) that was cooled to −78 °C. The reaction mixture was allowed to warm slowly to 0 °C, then it was warmed rapidly to 20 °C and vacuum-filtered through a fritted glass disk. The solvent was evaporated from the filtrate, and the orange solid residue was dried for 12 h in high vacuum. The crude product was recrystallized from Et$_2$O/hexanes (1:3) to give the amber stanna[1]ferrocenophane **7b** (1.43 g, 85 %). ^{1}H NMR (200 MHz, $CDCl_3$, 20 °C): $\delta = 6.93$ (s/d, $J(^{117/119}\mathrm{Sn},\mathrm{H}) = 21$ Hz, 4H; *m*-Mes), 4.36 (pst, J(H,H) = 2 Hz, 4H; Cp), 4.23 (pst, J(H,H) = 2 Hz, 4H; Cp), 2.71 (s/d, $J(^{117/119}\mathrm{Sn},\mathrm{H}) = 7$ Hz, 12H; *o*-Me), 2.28 (br, 6H; *p*-Me); ^{13}C NMR (75.5 MHz, $CDCl_3$, 20 °C): $\delta = 145.3$ ($J(^{117/119}\mathrm{Sn},^{13}\mathrm{C}) = 40$ Hz; *o*-Mes), 139.3 ($J(^{117/119}\mathrm{Sn},^{13}\mathrm{C}) = 11$ Hz; *p*-Mes), 135.7 ($J(^{119}\mathrm{Sn},^{13}\mathrm{C}) = 578$ Hz, $J(^{117}\mathrm{Sn},^{13}\mathrm{C}) = 552$ Hz; *ipso*-Mes), 128.5 ($J(^{117/119}\mathrm{Sn},^{13}\mathrm{C}) = 50$ Hz; *m*-Mes), 77.0 ($J(^{117/119}\mathrm{Sn},^{13}\mathrm{C}) = 51$ Hz; Cp), 75.7 ($J(^{117/119}\mathrm{Sn},^{13}\mathrm{C}) = 38$ Hz; Cp), 38.2 ($J(^{119}\mathrm{Sn},^{13}\mathrm{C}) = 412$ Hz, $J(^{117}\mathrm{Sn},^{13}\mathrm{C}) =$ 395 Hz; *ipso*-Cp), 25.1 ($J(^{117/119}\mathrm{Sn},^{13}\mathrm{C}) = 41$ Hz; *o*-Me), 21.0 (*p*-Me); ^{119}Sn NMR (111.8 MHz, $CDCl_3$, 20 °C): $\delta = -128.3$; UV/Vis (THF): λ_{max} (ε) = 420 (90), 481 (176); MS (70 eV, EI): *m/z* (%): 542 (100) [M^+], 423 (44) [M^+ − Mes], 305 (60) [$M^+ - 2$Mes]; $C_{28}H_{30}$FeSn (541.1): calcd C 62.15, H 5.59; found C 61.81, H 5.67; DSC: polymerization exotherm 160 °C (peak), 142 °C (onset), $\Delta H = -18(10)$ kJ mol^{-1}.

ROP of 7b and synthesis of 8b: The poly(ferrocenylstannane) **8b** was obtained from **7b** in two ways.

Thermal ROP: Solid-state polymerization was carried out by heating crystalline **7b** (typically 2.0 g) in a sealed evacuated Pyrex tube at 180 °C for 6 h. Monomodal high-molecular-weight poly(ferrocenylstannane) **8b** was formed in a quantitative yield.

ROP in solution: When **7b** (20 mg, 37 μmol) was dissolved in benzene (0.6 mL) 50 % conversion was detected over 15 days giving polymeric material **8b** (95 %), which was shown to have a very high molecular weight, and the cyclic dimer **3** (ER$_x$ = SnMes$_2$) (5 %). In $CHCl_3$, a larger amount (20–30 %) of dimer **3** (ER$_x$ = SnMes$_2$) was formed over a period of 15 days in addition to approximately 20 % of very low-molecular-weight material ($M_n < 1000$ according to a GPC analysis; the most notable feature in the ^{1}H NMR spectrum in $CDCl_3$ was a singlet at $\delta = 4.10$, which is indicative of an unsubstituted or deuterated Cp ring). For **8b**: ^{1}H NMR (300 MHz, $CDCl_3$, 40 °C): $\delta = 6.76$ (s/d, $J(^{117/119}\mathrm{Sn},\mathrm{H}) = 17$ Hz, 4H; *m*-Mes), 4.10 (br, 4H; Cp), 4.05 (br, 4H; Cp), 2.25 (s, 6H; *p*-Me), 2.10 (s, 12H; *o*-Me); ^{13}C NMR (75.5 MHz, $CDCl_3$, 40 °C): $\delta = 143.9$ ($J(^{117/119}\mathrm{Sn},^{13}\mathrm{C}) = 35$ Hz; *o*-Mes), 140.5, 137.5 (*ipso*-*p*-Mes), 128.2 ($J(^{117/119}\mathrm{Sn},^{13}\mathrm{C}) = 45$ Hz; *m*-Mes), 74.9 ($J(^{117/119}\mathrm{Sn},^{13}\mathrm{C}) = 53$ Hz; Cp), 74.4 ($J(^{119}\mathrm{Sn},^{13}\mathrm{C}) = 537$ Hz, $J(^{117}\mathrm{Sn},^{13}\mathrm{C}) =$ 512 Hz; *ipso*-Cp), 72.1 ($J(^{117/119}\mathrm{Sn},^{13}\mathrm{C}) = 40$ Hz; Cp), 26.1 ($J(^{117/119}\mathrm{Sn},^{13}\mathrm{C}) = 33$ Hz; *o*-Me), 21.1 (*p*-Me); ^{119}Sn NMR (111.8 MHz, $CDCl_3$, 40 °C): $\delta = -127.0$; pyrolysis MS (70 eV, EI, 400 °C): *m/z* (%): 661 (6) [(η-C_5H_5)Fe(η-C_5H_4SnMes$_3$)$^+$], 542 (11) [(η-C_5H_4)Fe(η-C_5H_4SnMes$_2$)$^+$], 478 (18) [Fe(η-C_5H_4SnMes$_2$)$^+$], 186 (27) [Fe(η-$C_5H_5)_2^+$]; pyrolysis MS (70 eV, EI, 450 °C): *m/z* (%): 1203 (3) [(η-C_5H_4)Fe(η-C_5H_4SnMes$_2\eta$-C_5H_4)Fe(η-C_5H_4SnMes$_3$)$^+$], 1138 (5) [(SnMes$_3\eta$-C_5H_4)Fe(η-C_5H_4SnMes$_3$)$^+$], 1084 (7) [(η-C_5H_4)Fe(η-C_5H_4SnMes$_2\eta$-C_5H_4)Fe(η-C_5H_4SnMes$_2$)$^+$] [M^+], 965 (16) [M^+ − Mes], 846 (73) [$M^+ - 2$Mes], 661 (87) [(η-C_5H_4)Fe(η-

$C_5H_4SnMes_3)^+$], 542 (100) [$(\eta$-$C_5H_4)Fe(\eta$-$C_5H_4SnMes_2)^+$]; UV/Vis (THF): λ_{max} (ε) = 445 (227); $[C_{28}H_{30}FeSn]_n$ ([541.1]$_n$): calcd C 62.15, H 5.59; found C 60.74, H 5.57; DSC: T_g = 208 °C (ΔC_p = 60(10) J mol^{-1}); GPC (THF, versus polystyrene): thermal polymerization: M_n = 82000 (PDI = 1.9); polymerization in solution (20 °C): $CHCl_3$, M_n < 1000; benzene, M_n = 1050000 (PDI = 1.3).

Reactions of dilithioferrocene·2/3TMEDA with $MesSnCl_3$, *n*BuMesSnCl$_2$, and PhMesSnCl$_2$: In a similar manner to the synthesis of **7b**, reactions of $MesSnCl_3$, *n*BuMesSnCl$_2$, and PhMesSnCl$_2$ with dilithioferrocene·2/3TMEDA were attempted at low temperature. Although the formation of a red product could be observed at −30 °C, crystallization of the products from the reaction mixture (analogous to the isolation of **7a**) or work-up at 20 °C (analogous to the isolation of **7b**) failed because the monomers tended to polymerize, even at low temperature.

Synthesis of cyclic dimer 3 (ER$_x$ = Sn*t*Bu$_2$): Compound **7a** (2.00 g, 4.80 mmol) was dissolved in CH_2Cl_2 (50 mL) and the resulting solution was stirred at ambient temperature under a N_2 atmosphere for 8 h. The polymeric product **8a** was precipitated into hexanes. The solvent was removed under vacuum from the remaining solution, which contained **3** (ER$_x$ = Sn*t*Bu$_2$) and low-molecular-weight **8a**. A toluene solution of this mixture was passed through a small amount of alumina (weakly basic, Brockman I., 150 mesh) to remove low-molecular-weight poly(ferrocenylstannane). Recrystallization from toluene resulted in the isolation of amber-orange crystalline distanna[1,1]ferrocenophane **3** (ER$_x$ = Sn*t*Bu$_2$) (650 mg, 32 % yield based on stanna[1]ferrocenophane **7a**). For **3** (ER$_x$ = Sn*t*Bu$_2$): ^{1}H NMR (200 MHz, $CDCl_3$, 20 °C): δ = 4.41 (pst, J(H,H) = 2 Hz, 8H; Cp), 4.18 (pst, J(H,H) = 2 Hz, 8H; Cp), 1.18 (s/d, $J(^{117/119}Sn,H)$ = 64 Hz, 36H; *t*Bu); ^{13}C NMR (50.3 MHz, $CDCl_3$, 20 °C): δ = 75.2 ($J(^{117/119}Sn,^{13}C)$ = 40 Hz; Cp), 70.2 ($J(^{117/119}Sn,^{13}C)$ = 34 Hz; Cp), 69.2 ($J(^{117}Sn,^{13}C)$ = 368 Hz, $J(^{119}Sn,^{13}C)$ = 385 Hz; *ipso*-Cp), 31.3 ($J(^{117}Sn,^{13}C)$ = 390 Hz, $J(^{119}Sn,^{13}C)$ = 408 Hz; *t*Bu), 28.1 (*ipso*-*t*Bu); ^{119}Sn NMR (111.8 MHz, $CDCl_3$, 20 °C): δ = −33.3; MS (70 eV, EI): *m/z* (%): 836 (2) [M^+], 779 (73) [$M^+ - t$Bu], 665 (67) [$M^+ - 3t$Bu], 608 (57) [$M^+ - 4t$Bu], 368 (100) [$M^+ - 2$Sn*t*Bu$_2$], 304 (58) [Fe(η-$C_5H_4)_2Sn^+$]; $C_{36}H_{52}Fe_2Sn_2$ (833.9): calcd C 51.85, H 6.29; found C 52.45, H 6.09.

Synthesis of 3 (ER$_x$ = SnMes$_2$): Compound **7b** (1.00 g, 1.85 mmol) was dissolved in $CHCl_3$ (50 mL) and the resulting solution was heated under reflux for 1 day. The polymeric product **8b** was precipitated into hexanes. The solvent was removed under vacuum from the remaining solution, which contained **3** (ER$_x$ = SnMes$_2$) and low-molecular-weight **8b**. A toluene solution of this mixture was passed through a small amount of alumina (weakly basic, Brockman I., 150 mesh) to remove low-molecular-weight poly(ferrocenylstannane). Recrystallization from toluene resulted in the isolation of orange crystalline distanna[1,1]ferrocenophane **3** (ER$_x$ = SnMes$_2$)·toluene (240 mg, 22 % based on stanna[1]ferrocenophane **7b**). For **3** (ER$_x$ = SnMes$_2$): ^{1}H NMR (300 MHz, $CDCl_3$, 20 °C): δ = 6.77 (s/d, $J(^{117/119}Sn,H)$ = 17 Hz, 8H; *m*-Mes), 4.34 (br, 8H; Cp), 4.20 (pst, J(H,H) = 2 Hz, 8H; Cp), 2.25 (br, 36H; *o*-Me, *p*-Me); ^{13}C NMR (50.3 MHz, $CDCl_3$, 20 °C): δ = 144.2 ($J(^{117/119}Sn,^{13}C)$ = 33 Hz; *o*-Mes), 140.7 (*ipso*-Mes), 137.7 ($J(^{117/119}Sn,^{13}C)$ = 11 Hz; *p*-Mes), 128.0 ($J(^{117/119}Sn,^{13}C)$ = 45 Hz; *m*-Mes), 76.7 (unresolved; Cp), 74.1 (unresolved; *ipso*-Cp), 71.0 ($J(^{117/119}Sn,^{13}C)$ = 47 Hz; Cp), 26.2 ($J(^{117/119}Sn,^{13}C)$ = 32 Hz; *o*-Me), 21.0 (*p*-Me); ^{119}Sn NMR (111.8 MHz, $CDCl_3$, 20 °C): δ = −111.5; MS (70 eV, EI): *m/z* (%): 1084 (76) [M^+], 965 (57) [M^+ − Mes], 608 (11) [(Fe(η-$C_5H_4)_2Sn)_2^+$], 542 (18) [M^{2+}]/[M^+ − Fe(η-$C_5H_4)_2SnMes_2$], 423 (59) [Fe(η-$C_5H_4)_2SnMes^+$], 304 (55) [Fe(η-$C_5H_4)_2Sn^+$], 119 (100) [*M*es$^+$]; $C_{63}H_{68}Fe_2Sn_2$ (1082.2)·C_7H_8 (92.1): calcd C 64.43, H 5.83; found C 64.39, H 5.78.

Synthesis of 9: A solution of Pt(1,5-cod)$_2$ (58 mg, 0.14 mmol) in toluene (1.5 mL) was added slowly to a solution of **7a** (60 mg, 0.14 mmol) in toluene (1.5 mL). The reaction solution was stirred for 3 h, then passed through a small amount of alumina (weakly basic, Brockman I., 150 mesh) and the toluene was removed under vacuum. Crystallization of the product from toluene/hexanes (4 mL, 1:4) at −55 °C resulted in the isolation of **9** (60 mg, 60 %) as amber crystals. In toluene solution at ambient temperature **9** was found to decompose slowly. ^{1}H NMR (300 MHz, C_6D_6, 20 °C): δ = 5.33 (m, $J(^{195}Pt,H)$ = 45 Hz, 2H; $-C_2H_2-$), 5.06 (m, $J(^{195}Pt,H)$ = 37 Hz, 2H; $-C_2H_2-$), 4.71 (pst, J(H,H) = 2 Hz, 2H; Cp), 4.46 (pst, J(H,H) = 2 Hz, 2H; Cp), 4.37 (pst, J(H,H) = 2 Hz, 2H; Cp), 4.07 (pst, J(H,H) = 2 Hz, $J(^{195}Pt,H)$ = 29 Hz, 2H; α-Cp−Pt), 1.77 (m, 8H; $-C_2H_4-$), 1.55 (s/d, $J(^{117/119}Sn,H)$ = 57 Hz, 18H; CH_3); ^{13}C NMR (100.6 MHz, C_6D_6, 20 °C): δ = 117.3 ($J(^{195}Pt,^{13}C)$ = 46 Hz; CH), 90.3 ($J(^{195}Pt,^{13}C)$ = 70 Hz; CH), 78.4 ($J(^{195}Pt,^{13}C)$ = 98 Hz, $J(^{117/119}Sn,^{13}C)$ = 280 Hz; *ipso*-Cp−Sn), 76.9 ($J(^{117/119}Sn,^{13}C)$ = 36 Hz; β-Cp−Sn), 74.2 ($J(^{195}Pt,^{13}C)$ = 1055 Hz, $J(^{117/119}Sn,^{13}C)$ = 19 Hz; *ipso*-Cp−Pt), 72.6 ($J(^{195}Pt,^{13}C)$ = 67 Hz; β-Cp−Pt), 70.3 ($J(^{195}Pt,^{13}C)$ = 67 Hz; α-Cp−Pt), 70.1 $J(^{117/119}Sn,^{13}C)$ = 28 Hz; α-Cp−Sn), 33.4 ($J(^{195}Pt,^{13}C)$ = 123 Hz, $J(^{117/119}Sn,^{13}C)$ = 253 Hz; *ipso*-*t*Bu), 33.2 ($J(^{195}Pt,^{13}C)$ = 5 Hz; *t*Bu), 31.6 ($J(^{195}Pt,^{13}C)$ = 8 Hz; CH_2), 27.8 ($J(^{195}Pt,^{13}C)$ = 6 Hz; CH_2); ^{119}Sn NMR (111.8 MHz, C_6D_6, 20 °C): δ = 20.1 ($J(^{195}Pt,^{119}Sn)$ = 14640 Hz); ^{195}Pt NMR (64.2 MHz, C_6D_6, 20 °C): δ = −3604 ($J(^{195}Pt,^{119}Sn)$ = 14640 Hz, $J(^{195}Pt,^{117}Sn)$ = 13991 Hz); MS (FAB): *m/z* (%): 721 (20) [M^+], 664 (77) [$M^+ - t$Bu], 605 (18) [$M^+ - 2t$Bu], 499 (44) [Fe(η-$C_5H_4)_2PtSn^+$], 186 (100) [Fe(η-$C_5H_5)_2^+$]; $C_{26}H_{38}FePtSn$ (720.2): calcd C 43.36, H 5.32; found C 43.84, H 5.23.

Attempted transition-metal-catalyzed ROP of 7a and 7b with Pt$_2$(η-CH$_2$CHSiMe$_2$OSiMe$_2\eta$-CHCH$_2$)$_3$: When **7a** (20 mg, 48 μmol) in C_6D_6 (0.5 mL) was treated with Pt$_2$(η-CH_2CHSiMe$_2$OSiMe$_2\eta$-CHCH$_2$)$_3$ (0.5 μL of a 3 % solution in xylenes, Karstedt's catalyst), a dramatic decrease in the rate of ROP, compared with the solution ROP of **7a** in C_6D_6, was noted. However, after 4 days almost all the **7a** was consumed and high-molecular-weight polymer **8a** (M_n = 800000, PDI = 1.8) was formed. An ROP reaction of **7a** (1.00 g, 2.40 mmol) in toluene (10 mL) with Karstedt's catalyst (12.5 μL of a 3 % solution in xylenes) only proceeded to 50 % conversion after being heated at 110 °C for 6 h, to form high-molecular-weight polymer (M_n = 400000, PDI = 2.2).

A similar result was obtained, when **7b** (20 mg, 37 μmol) in C_6D_6 (0.5 mL) was treated with Karstedt's catalyst (5 μL of a 3 % solution in xylenes). Over a period of 30 days only 30 % of the monomer **7b** was consumed, forming **8b** (M_n = 50000, PDI = 1.1).

Crystal structure determinations for 3 (ER$_x$ = Sn*t*Bu$_2$, SnMes$_2$), 7a, 7b, and 9: Crystal data and details of the measurements are summarized in Table 9. The structures were solved by direct methods (SHELXS97) and refined by full-matrix least squares (SHELXL97) based on F^2 with all reflections. Non-hydrogen atoms were refined anisotropically, and hydrogen atoms were included in calculated positions.

Crystallographic data (excluding structure factors) for the structures reported in this paper have been deposited with the Cambridge Crystallographic Data Centre as supplementary publication no. CCDC-101299. Copies of the data can be obtained free of charge on application to CCDC, 12 Union Road, Cambridge CB2 1EZ, UK (fax: (+44) 1223-336-033; e-mail: deposit@ccdc.cam.ac.uk).

Acknowledgments: We thank the donors of the Petroleum Research Fund (PRF), administered by the American Chemical Society, for financial support of this work. We also acknowledge a DFG postdoctoral fellowship for F.J. and an Ontario Graduate Student Fellowship for R.R.. I.M. is grateful to the Alfred P. Sloan Foundation for a Research Fellowship (1994 – 1998), to NSERC for an E.W.R. Steacie Fellowship (1997 – 1999), and to the University of Toronto for a McLean Fellowship (1997 – 2003). We thank Prof. J. Sheridan and K. Temple for providing the Pt(1,5-cod)$_2$, R. Perry for obtaining the Mössbauer data, and M. J. MacLachlan for recording the WAXS data.

Received: March 25, 1998 [F1063]

[1] Recent reviews: a) C. U. Pittman, C. E. Carraher, M. Zeldin, J. E. Sheats, B. M. Culbertson, *Metal-Containing Polymeric Materials*, Plenum, New York, **1996**; b) I. Manners, *Angew. Chem.* **1996**, *108*, 1712; *Angew. Chem. Int. Ed. Engl.* **1996**, *35*, 1602.

[2] Selected references: a) M. E. Wright, M. S. Sigman, *Macromolecules* **1992**, 25, 6055; b) H. B. Fyfe, M. Mlekuz, D. Zargarian, N. J. Taylor, T. B. Marder, *J. Chem. Soc. Chem. Commun.* **1991**, 188; c) H. W. Roesky, M. Lücke, *Angew. Chem.* **1989**, *101*, 480; *Angew. Chem. Int. Ed. Engl.* **1989**, *28*, 493; d) S. J. Davies, B. F. G. Johnson, M. S. Khan, J. Lewis, *J. Chem. Soc. Chem. Commun.* **1991**, 187; e) K. C. Sturge, A. D. Hunter, R. McDonald, B. D. Santarsiero, *Organometallics* **1992**, *11*, 3056; f) T. P. Pollagi, T. C. Stoner, R. F. Dallinger, T. M. Gilbert, M. D. Hopkins, *J. Am. Chem. Soc.* **1991**, *113*, 703; g) P. F. Brandt, T. B. Rauchfuss, *J. Am. Chem. Soc.* **1992**, *114*, 1926; h) R. Bayer, T. Pöhlmann, O. Nuyken, *Makromol. Chem. Rapid Commun.* **1993**, 14, 359; i) A. A. Dembek, P. J. Fagan, M. Marsi, *Macromolecules*, **1993**, 26, 2992; j) A. M. Gilbert, T. J. Katz, W. E. Geiger, M. P. Robben,

  0947-6539/98/0411-2126 $ 17.50+.50/0

Table 9. Crystal data and structure refinement.

	3 ($ER_x = SntBu_2$)	**3 · toluene** ($ER_x = SnMes_2$)	**7a**	**7b**	**9**
formula	$C_{36}H_{52}Fe_2Sn_2$	$C_{63}H_{68}Fe_2Sn_2$	$C_{18}H_{26}FeSn$	$C_{28}H_{30}FeSn$	$C_{26}H_{38}FePtSn$
M_r	833.86	1174.25	416.93	541.06	720.19
T, [K]	173(2)	293(2)	293(2)	150(2)	173(2)
wavelength, [Å]	$\lambda(Mo_{K\alpha}) = 0.71073$	$\lambda(Mo_{K\alpha}) = 0.71073$	$\lambda(Mo_{K\alpha}) = 0.71073$	$\lambda(Mo_{K\alpha}) = 0.71073$	$\lambda(Mo_{K\alpha}) = 0.71073$
crystal system	triclinic	orthorhombic	tetragonal	monoclinic	triclinic
space group	$P\bar{1}$	$Pbcn$	$P\bar{4}2_1c$	$P2_1/c$	$P\bar{1}$
a [Å]	8.391(2)	19.972(1)	19.667(2)	17.687(1)	9.948(1)
b [Å]	10.542(1)	16.289(1)	19.667(2)	12.402(1)	10.278(1)
c [Å]	10.978(1)	25.860(1)	9.0997(8)	32.064(1)	13.833(2)
α [°]	86.920(9)	90	90	90	88.582(9)
β [°]	69.70(1)	90	90	93.67(1)	80.205(9)
γ [°]	70.73(1)	90	90	90	61.915(8)
V [Å^3]	857.7(2)	5159.6(3)	3519.7(6)	7019.0(7)	1227.1(2)
Z	1	4	8	12	2
ρ_{calcd} [g cm^{-3}]	1.614	1.512	1.574	1.536	1.949
$\mu(Mo_{K\alpha})$ [mm^{-1}]	2.291	1.548	2.233	1.700	7.289
$F(000)$	420	2392	1680	3288	696
crystal size [mm]	$0.26 \times 0.23 \times 0.18$	$0.12 \times 0.11 \times 0.10$	$0.08 \times 0.08 \times 0.50$	$0.21 \times 0.18 \times 0.17$	$0.36 \times 0.33 \times 0.28$
diffractometer	Siemens P4	Kappa-CCD	Siemens P4	Kappa-CCD	Siemens P4
scan type, range	ω, 0.66	ϕ, 1	ω, 0.45	ϕ, 1	ω, 0.53
θ range [°]	2.74–30.00	2.04–26.37	2.93–27.00	1.27–27.00	2.56–30.00
limiting indices	$0 \le h \le 11$	$-24 \le h \le 24$	$0 \le h \le 25$	$-27 \le h \le 27$	$0 \le h \le 13$
	$-13 \le k \le 14$	$-20 \le k \le 20$	$0 \le k \le 25$	$-18 \le k \le 18$	$-12 \le k \le 14$
	$-14 \le l \le 15$	$-19 \le l \le 19$	$0 \le l \le 11$	$-48 \le l \le 48$	$-19 \le l \le 19$
reflns collected	5319	36993	4225	27615	7529
independent reflns	5004 ($R_{int} = 0.0284$)	5268 ($R_{int} = 0.0347$)	2158 ($R_{int} = 0.0360$)	14602 ($R_{int} = 0.0514$)	7149 ($R_{int} = 0.0313$)
abs. correction	empirical, psi-scan	empirical, redundant data	integration	empirical, redundant data	empirical, psi-scans
min. and max. transmission coeff.	0.4587–0.7175	0.8606–0.8360	0.7876–0.8422	0.7167–0.7610	0.2710–0.5925
data / parameters	5004/286	5267/311	2158/192	13260/829	7149/415
GoF on F^2	0.946	1.025	0.864	0.827	1.003
$R1$[a] [$I > 2\sigma(I)$]	0.0357	0.0221	0.0267	0.0365	0.0275
$wR2$[b] (all data)	0.0813	0.0695	0.0473	0.0833	0.0684
ext. coefficient	0.0008(5)	0.00034(5)	0.00029(2)	none	0.0012(2)
peak/hole [e Å^{-3}]	1.071/ −1.080	0.838/ −0.506	0.274/ −0.321	1.038/ −1.034	1.410/ −1.733

[a] $R1 = \Sigma||F_o| - |F_c||/\Sigma|F_o|$; [b] $wR2 = \{\Sigma[w(F_o^2 - F_c^2)^2]/\Sigma[w(F_o^2)^2]\}^{1/2}$.

A. L. Rheingold, *J. Am. Chem. Soc.* **1993**, *115*, 3199; k) H. M. Nugent, M. Rosenblum, P. Klemarczyk, *J. Am. Chem. Soc.* **1993**, *115*, 3848; l) G. E. Southard, M. D. Curtis, *Organometallics* **1997**, *16*, 5618; m) S. S. Zhu, T. M. Swager, *J. Am. Chem. Soc.* **1997**, *119*, 12568; n) D. L. Compton, P. F. Brandt, T. B. Rauchfuss, D. F. Rosenbaum, C. F. Zukoski, *Chem. Mater.* **1995**, *7*, 2342; o) M. A. Buretea, T. D. Tilley, *Organometallics* **1997**, *16*, 1507; p) S. S. H. Mao, F.-Q. Liu, T. D. Tilley, *J. Am. Chem. Soc.* **1998**, *120*, 1193.

[3] a) D. A. Foucher, B.-Z. Tang, I. Manners, *J. Am. Chem. Soc.* **1992**, *114*, 6246; b) Y. Ni, R. Rulkens, I. Manners, *J. Am. Chem. Soc.* **1996**, *118*, 4102; c) P. Gómez-Elipe, P. M. Macdonald, I. Manners, *Angew. Chem.* **1997**, *109*, 780; *Angew. Chem. Int. Ed. Engl.* **1997**, *36*, 762; d) R. Resendes, P. Nguyen, A. J. Lough, I. Manners, *Chem. Commun.* **1998**, 1001.

[4] a) I. Manners, *Adv. Organomet. Chem.* **1995**, *37*, 131; b) R. Rulkens, A. J. Lough, I. Manners, S. R. Lovelace, C. Grant, W. E. Geiger, *J. Am. Chem. Soc.* **1996**, *118*, 12683; c) R. Rulkens, R. Resendes, A. Verma, I. Manners, K. Murti, E. Fossum, P. Miller, K. Matyjaszewski, *Macromolecules* **1997**, *30*, 8165; d) X.-H. Liu, D. W. Bruce, I. Manners, *Chem. Commun.* **1997**, 289; e) M. J. MacLachlan, P. Aroca, N. Coombs, I. Manners, G. A. Ozin, *Adv. Mater.* **1998**, *10*, 144; f) I. Manners, *Can. J. Chem.* **1998**, *76*, 731.

[5] a) M. Tanaka, T. Hayashi, *Bull. Chem. Soc. Jpn.* **1993**, *66*, 334; b) M. Hmyene, A. Yassar, M. Escorne, A. Percheron-Guegan, F. Garnier, *Adv. Mater.* **1994**, *6*, 564; c) S. Barlow, A. L. Rohl, S. Shi, C. M. Freeman, D. O'Hare, *J. Am. Chem. Soc.* **1996**, *118*, 7578; d) K. H. Pannell, V. V. Dement'ev, H. Li, F. Cervantes-Lee, M. T. Nguyen, A. Diaz, *Organometallics* **1994**, *13*, 3644; e) K. Mochida, N. Shibayama, M. Goto, *Chem. Lett.* **1998**, 339.

[6] E. W. Neuse, H. Rosenberg, *J. Macromol. Sci. C* **1970**, *4*, 110.

[7] A. G. Osborne, R. H. Whiteley, *J. Organomet. Chem.* **1975**, *101*, C27.

[8] a) H. Stoeckli-Evans, A. G. Osborne, R. H. Whiteley, *J. Organomet. Chem.* **1980**, *194*, 91; b) A. G. Osborne, R. H. Whiteley, R. E. Meads, *J. Organomet. Chem.* **1980**, *193*, 345.

[9] D. Seyferth, H. P. Withers, *Organometallics* **1982**, *1*, 1275.

[10] I. R. Butler, W. R. Cullen, F. W. B. Einstein, S. J. Rettig, A. J. Willis, *Organometallics* **1983**, *2*, 128.

[11] R. Broussier, A. Da Rold, B. Gautheron, Y. Dromzee, Y. Jeannin, *Inorg. Chem.* **1990**, *29*, 1817.

[12] R. Broussier, A. Da Rold, B. Gautheron, *J. Organomet. Chem.* **1992**, *427*, 231.

[13] T.-Y. Dong, M.-Y. Hwang, Y.-S. Wen, W.-S. Hwang, *J. Organomet. Chem.* **1990**, *391*, 377

[14] V. V. Dement'ev, F. Cervantes-Lee, L. Parkanyi, H. Sharma, K. H. Pannell, M. T. Nguyen, A. Diaz, *Organometallics* **1993**, *12*, 1983.

[15] D. A. Foucher, C. H. Honeyman, J. M. Nelson, B. Z. Tang, I. Manners, *Angew. Chem.* **1993**, *105*, 1843; *Angew. Chem. Int. Ed. Engl.* **1993**, *32*, 1709.

[16] a) J. K. Pudelski, D. P. Gates, R. Rulkens, I. Manners, *Angew. Chem.* **1995**, *107*, 1633; *Angew. Chem. Int. Ed. Engl.* **1995**, *34*, 1506; b) R. Rulkens, D. P. Gates, D. Balaishis, J. K. Pudelski, D. F. McIntosh, A. J. Lough, I. Manners, *J. Am. Chem. Soc.* **1997**, *119*, 10976.

[17] H. Braunschweig, R. Dirk, M. Müller, P. Nguyen, R. Resendes, D. P. Gates, I. Manners, *Angew. Chem.* **1997**, *109*, 2433; *Angew. Chem. Int. Ed. Engl.* **1997**, *36*, 2338.

[18] A. Clearfield, C. J. Simmons, H. P. Withers, D. Seyferth, *Inorg. Chim. Acta* **1983**, *75*, 139.

[19] M. Herberhold, U. Steffl, W. Milius, B. Wrackmeyer, *Angew. Chem.* **1996**, *108*, 1927; *Angew. Chem. Int. Ed. Engl.* **1996**, *35*, 1803.

[20] W. A. Herrmann, M. J. A. Morawietz, H.-F. Herrmann, F. Küber, *J. Organomet. Chem.* **1996**, *509*, 115.
[21] R. Rulkens, A. J. Lough, I. Manners, *Angew. Chem.* **1996**, *108*, 1929; *Angew. Chem. Int. Ed. Engl.* **1996**, *35*, 1805.
[22] Alternative names for these polymers include poly(ferrocenylenestannane)s and poly(ferrocenediylstannane)s; the abbreviation Cp in this manuscript refers to substituted and unsubstituted cyclopentadienyl ligands.
[23] High-molecular-weight polymers with tin in the backbone are very rare. For the recent synthesis of poly(stannane)s $[SnR_2]_n$ see: a) T. Imori, V. Lu, H. Cai, T. D. Tilley, *J. Am. Chem. Soc.* **1995**, *117*, 9931; b) N. Devylder, M. Hill, K. C. Molloy, G. J. Price, *Chem. Commun.* **1996**, 711.
[24] D. A. Foucher, Ph.D. Thesis, University of Toronto, **1993**.
[25] This is also expected on the basis of the large covalent radius of tin (140 pm) compared with those of germanium (122 pm) and silicon (118 pm).
[26] a) R. F. Bryan, *J. Chem. Soc. (A)* **1967**, 192; b) F. W. B. Einstein, R. Restivo, *Inorg. Chim. Acta* **1971**, *5*, 501; c) M. Veith, L. Stahl, V. Huch, *Organometallics* **1993**, *12*, 1914.
[27] a) J. Silver, *J. Chem. Soc. Dalton Trans.* **1990**, 3513; b) D. A. Foucher, M. Edwards, R. A. Burrow, A. J. Lough, I. Manners, *Organometallics* **1994**, *13*, 4959.
[28] Y. S. Sohn, D. N. Hendrickson, H. B. Gray, *J. Am. Chem. Soc.* **1971**, *93*, 3603.
[29] The ε_{max} value for the recently synthesized thia[1]ferrocenophane, which has an α ring tilt of 31°, was found to be $578\,M^{-1}cm^{-1}$; see Ref. [16b].
[30] Attempts to obtain single crystals of poly(ferrocenylstannane) **8a** by ROP in the solid state from single crystals of **7a** resulted in only partially crystalline **8a**.
[31] J. K. Pudelski, D. A. Foucher, C. H. Honeyman, P. M. Macdonald, I. Manners, S. Barlow, D. O'Hare, *Macromolecules* **1996**, *29*, 1894.
[32] J. Park, Y. Seo, S. Cho, D. Whang, K. Kim, T. Chang, *J. Organomet. Chem.* **1995**, *489*, 23.
[33] D. L. Zechel, D. A. Foucher, J. K. Pudelski, G. P. A. Yap, A. L. Rheingold, I. Manners, *J. Chem. Soc. Dalton Trans.* **1995**, 1893.
[34] R. Petersen, D. A. Foucher, B.-Z. Tang, A. J. Lough, N. P. Raju, J. E. Greedan, I. Manners, *Chem. Mater.* **1995**, *7*, 2045.
[35] J. K. Pudelski, D. A. Foucher, C. H. Honeymann, A. J. Lough, I. Manners, S. Barlow, D. O'Hare, *Organometallics* **1995**, *14*, 2470.
[36] I. Manners, *J. Inorg. Organomet. Polym.* **1993**, *3*, 185.
[37] R. Rulkens, A. J. Lough, I. Manners, *J. Am. Chem. Soc* **1994**, *116*, 797.
[38] M. T. Nguyen, A. F. Diaz, V. V. Dement'ev, K. H. Pannell, *Chem. Mater.* **1993**, *5*, 1389.
[39] A. F. Diaz, U. T. Müller-Westerhoff, A. Nazzal, M. Tanner, *J. Organomet. Chem.* **1982**, *236*, C45.
[40] G. Utri, K.-E. Schwarzhans, G. M. Allmaier, *Z. Naturforsch.*, *B* **1990**, *45*, 755.
[41] a) Y. Ni, R. Rulkens, J. K. Pudelski, I. Manners, *Makromol. Chem. Rapid Commun.* **1995**, *14*, 637; b) N. P. Reddy, H. Yamashita, M. Tanaka, *J. Chem. Soc. Chem. Commun.* **1995**, 2263.
[42] J. B. Sheridan, K. Temple, A. J. Lough, I. Manners, *J. Chem. Soc. Dalton Trans.* **1997**, 711.
[43] Very recently the first 1,3-distanna-2-platina[3]ferrocenophane was reported to have been obtained by insertion of $[Pt(PPh_3)_2C_2H_4]$ into the Sn–Sn bond of the respective [2]ferrocenophane: M. Herberhold, U. Steffl, W. Milius, B. Wrackmeyer, *Angew. Chem.* **1997**, *109*, 1545; *Angew. Chem. Int. Ed. Engl.* **1997**, *36*, 1508.
[44] a) R. Gleiter, R. Seeger, *Helv. Chim. Acta* **1971**, *54*, 1217; b) U. Behrens, *J. Organomet. Chem.* **1979**, *182*, 89; c) W. E. Watts, *J. Organomet. Chem.* **1981**, *220*, 165; d) B. Wrackmeyer, U. Dörfler, W. Milius, M. Herberhold, *Polyhedron* **1995**, *14*, 1425; e) A. Appel, F. Jäkle, T. Priermeier, R. Schmid, M. Wagner, *Organometallics* **1996**, *15*, 1188.
[45] Of 52 Pt–Sn bonds found in the Cambridge database, 44 were in a range from 2.475 to 2.750 Å. For selected examples, see: a) V. G. Albano, C. Castellari, V. De Felice, A. Panunzi, F. Ruffo, *J. Organomet. Chem.* **1992**, *425*, 177; b) H. C. Clark, G. Ferguson, M. J. Hampden-Smith, H. Ruegger, B. L. Ruhl, *Can. J. Chem.* **1988**, *66*, 3120; c) L. A. Latif, C. Eaborn, A. P. Pidcock, N. G. Seik Weng, *J. Organomet. Chem.* **1994**, *474*, 217.
[46] M. S. Wrighton, M. C. Palazzotto, A. B. Bocarsly, J. M. Bolts, A. B. Fischer, L. Nadjo, *J. Am. Chem. Soc.* **1978**, *100*, 7264.
[47] J. J. Bishop, A. Davison, M. L. Katcher, R. E. Lichtenberg, J. C. Merrill, J. Smart, *J. Organomet. Chem.* **1971**, *27*, 241.
[48] I. R. Butler, W. R. Cullen, J. Ni, S. J. Rettig, *Organometallics* **1985**, *4*, 2196.
[49] H. Berwe, A. Haas, *Chem. Ber.* **1987**, *120*, 1175.
[50] P. Brown, M. F. Mahon, K. C. Molloy, *J. Organomet. Chem.* **1992**, *435*, 265.
[51] M. Weidenbruch, K. Schäfers, J. Schlaefke, K. Peters, H. G. von Schnering, *J. Organomet. Chem.* **1991**, *415*, 343.
[52] F. Jäkle, I. Manners, unpublished results.

  0947-6539/98/0411-2128 $ 17.50+.50/0